



MSU Graduate Theses

Spring 2022


The Role of the Host Factor SPTBN1 in HIV-1 Infection of Microglial Cells

Marc Gordon Havlicek

Missouri State University, Havlicek007@live.missouristate.edu

As with any intellectual project, the content and views expressed in this thesis may be considered objectionable by some readers. However, this student-scholar's work has been judged to have academic value by the student's thesis committee members trained in the discipline. The content and views expressed in this thesis are those of the student-scholar and are not endorsed by Missouri State University, its Graduate College, or its employees.

Follow this and additional works at: <https://bearworks.missouristate.edu/theses>

 Part of the [Immunology and Infectious Disease Commons](#), and the [Virus Diseases Commons](#)

Recommended Citation

Havlicek, Marc Gordon, "The Role of the Host Factor SPTBN1 in HIV-1 Infection of Microglial Cells" (2022). *MSU Graduate Theses*. 3709.
<https://bearworks.missouristate.edu/theses/3709>

This article or document was made available through BearWorks, the institutional repository of Missouri State University. The work contained in it may be protected by copyright and require permission of the copyright holder for reuse or redistribution.

For more information, please contact bearworks@missouristate.edu.

**THE ROLE OF THE HOST FACTOR SPTBN1 IN HIV-1 INFECTION OF
MICROGLIAL CELLS**

A Master's Thesis

Presented to

The Graduate College of
Missouri State University

In Partial Fulfillment

Of the Requirements for the Degree

Master of Science, Cell and Molecular Biology

By

Marc Gordan Havlicek

May 2022

THE ROLE OF THE HOST FACTOR SPTBN1 IN HIV-1 INFECTION OF MICROGLIAL CELLS

Biomedical Science

Missouri State University, May 2022

Master of Science

Marc Gordan Havlicek

ABSTRACT

HIV-1 is the etiological agent that cause AIDS. Since the 1980's when HIV-1 was discovered, much has been discovered, however a cure for HIV-1 has eluded researchers. Effective therapeutics do exist but can have adverse side effects including HAND/HAD which leads to neurodegeneration in patients regardless of viral suppression. One area of research that holds the possibility of discovering new viral targets and therapeutics is host factor interaction within the replication process. One host factor that can cause a decrease in HIV-1 infectivity is SPTBN1. SPTBN1 is a cytoskeletal protein that was shown to bind to the capsid and nucleocapsid proteins of HIV. However, the exact mechanism of SPTBN1 involvement in HIV-1 infection is still unknown. Here we utilized siRNA to downregulate SPTBN1 expression and ascertain the role it plays in HIV-1 infection. When SPTBN1 was downregulated, there was a 19.75% decrease in the infectivity of HIV-1. A mini-CsA washout assay was then performed to assay capsid uncoating at the early time points. At the 30 min time point there was a 9% decrease in uncoating and a decrease of 24% at 1hr when SPTBN1 expression was downregulated. From these results, the decrease in infectivity could be caused by the decrease in uncoating. However, it is still unknown if SPTBN1 plays a part in the other replication steps of HIV-1 and more research is needed to divulge the full role SPTBN1 plays in HIV-1 infection.

KEYWORDS: HIV-1, microglial cells, uncoating, SPTBN1, HAD/HAND, infectivity

**THE ROLE OF THE HOST FACTOR SPTBN1 IN HIV-1 INFECTION OF
MICROGLIAL CELLS**

By

Marc Gordan Havlicek

A Master's Thesis
Submitted to the Graduate College
Of Missouri State University
In Partial Fulfillment of the Requirements
For the Degree of Master of Science, Cell and Molecular Biology

May 2022

Approved:

Amy Hulme, Ph.D., Thesis Committee Chair

Randi Ulbricht, Ph.D., Committee Member

Richard Garrad, Ph.D., Committee Member

Julie Masterson, Ph.D., Dean of the Graduate College

In the interest of academic freedom and the principle of free speech, approval of this thesis indicates the format is acceptable and meets the academic criteria for the discipline as determined by the faculty that constitute the thesis committee. The content and views expressed in this thesis are those of the student-scholar and are not endorsed by Missouri State University, its Graduate College, or its employee.

ACKNOWLEDGEMENTS

I would like to thank the following people for their support during my graduate studies Dr Ulbricht and Dr. Garrad for their expertise. I want to give a special thanks to Dr. Hulme for her mentorship and guidance throughout my entire project.

TABLE OF CONTENTS

| | |
|--|---------|
| INTRODUCTION | Page 1 |
| Inflammation and Infected Cell Types | Page 2 |
| HIV-1 Virus, Proteins and Replication Cycle | Page 6 |
| Binding, Fusion, Uncoating and Reverse Transcription of HIV-1 | Page 11 |
| Nuclear Import, Integration and Production of Progeny Virions | Page 17 |
| SPTBN1 Structure and Function as a Host Factor For HIV-1 | Page 18 |
| The Role of the Cytoskeleton in HIV-1 Infection | Page 27 |
| Specific Aims and Hypothesis | Page 34 |
| MATERIAL AND METHODS | Page 37 |
| Culturing and Maintenance 293T and TCN14 cells | Page 37 |
| Making VSV-g-HIV-GFP Virus | Page 38 |
| Testing Infectivity of VSV-g Pseudotyped HIV-GFP Virus | Page 40 |
| SiRNA Knockdown of SPTBN1 | Page 41 |
| HIV-1 Infectivity of SPTBN1 Knockdown Cells | Page 42 |
| Mini-CsA Washout Assay and Construction of Primers | Page 44 |
| Confirmation of Primer and Determining Annealing Temperature SPTBN1 and GAPDH | Page 47 |
| Primer Efficacy and Confirming siRNA Knockdown | Page 47 |
| RESULTS | Page 52 |
| SPTBN1 Knockdown Effect on Infectivity | Page 52 |
| Confirming the Annealing Temperature of Primers | Page 54 |
| Determining Primer Efficacy for SPTBN1 and GAPDH | Page 55 |
| Confirming Knockdown of SPTBN1 | Page 61 |
| Determining the Effect of SPTBN1 Knockdown on Uncoating | Page 64 |
| DISCUSSION | Page 69 |
| Future Directions and Optimizing Knockdown | Page 74 |
| Full CsA Washout and Fusion Assay | Page 76 |
| WT HIV and VSV-g-HIV-GFP Difference | Page 78 |
| Viral Trafficking and TCN14 Cells Response to IL-27 | Page 79 |
| REFERENCES | Page 84 |

LIST OF TABLES

| | |
|---|---------|
| Table 1. Effects of HIV Infectivity in SPTBN1 Knockdown Cells | Page 53 |
| Table 2. Primer Efficacy of SPTBN1 Primers | Page 57 |
| Table 3. Primer Efficacy of GAPDH Primers | Page 59 |
| Table 4. Confirming Knockdown of SPTBN1 | Page 62 |
| Table 5. Confirming Knockdown using GAPDH | Page 63 |
| Table 6. Infectivity in SPTBN1 Knockdown Cells | Page 64 |
| Table 7. SPTBN1 Knockdown Affects on Uncoating. | Page 67 |

LIST OF FIGURES

| | |
|--|---------|
| Figure 1. Schematic of HIV-1 Dissemination Throughout the Body | Page 4 |
| Figure 2. Diagram of the HIV-1 Virion and Protein Location | Page 8 |
| Figure 3. Schematic of the Viral RNA Genome of HIV-1 | Page 9 |
| Figure 4. HIV-1 Replication Cycle | Page 11 |
| Figure 5. Capsid Core | Page 14 |
| Figure 6. The Strand Transfer of HIV-1 | Page 15 |
| Figure 7. Models of Uncoating | Page 17 |
| Figure 8. Spectrin Proteins | Page 25 |
| Figure 9. Microtubule Involvement with HIV-1 | Page 29 |
| Figure 10. Actin Treadmilling | Page 33 |
| Figure 11. Schematic of Knockdown Plate | Page 42 |
| Figure 12. Plate Setup of Testing Infectivity | Page 44 |
| Figure 13. Mini-Uncoating CsA Washout Assay | Page 46 |
| Figure 14. Primer Sequence | Page 47 |
| Figure 15. Orientation of KD Confirmation | Page 51 |
| Figure 16. Graph of Normalized Infectivity with SiRNA Knockdown | Page 53 |
| Figure 17. Annealing Temperature Confirmation for SPTBN1 and GAPDH Primers. | Page 55 |
| Figure 18. Amplification Curve for SPTBN1 Primers to Determine Primer Efficacy | Page 56 |
| Figure 19. Primer Efficacy Calculation and Graph of SPTBN1 Primers | Page 58 |
| Figure 20. Primer Efficacy Calculation and Graph of GAPDH Primers | Page 60 |
| Figure 21. Infectivity with SPTBN1 Knockdown | Page 64 |
| Figure 22. Mini-CsA Washout Assay Bar Graph | Page 68 |

INTRODUCTION

Human immunodeficiency virus 1 (HIV-1) is the etiologic agent that causes acquired immunodeficiency syndrome (AIDS; (1)). Since HIV-1 has been in the population, 38 million people are currently living with the virus and 33 million have expired due to AIDS (2, 3). AIDS is marked by the manifestation of multiple chronic infections, caused by the degradation of CD4⁺ T cells (4). When CD4⁺ T cells count decreases, the immune response to various pathological agents degrades, which ultimately leads to patient death (4, 5). Since the 1980s, when HIV-1 was discovered, much research has taken place to discover therapeutic agents, a cure for HIV-1 or a vaccine, but to date a cure or vaccine have eluded researchers (6, 7). However, a plethora of knowledge has been gained about HIV-1, to include viral factors and replication cycle of HIV-1, cellular factors aiding and inhibiting HIV-1, types of cells capable of facilitating infection, combination antiretroviral therapy (cART), and constant immune activation which leads to immune exhaustion and inflammation (1, 8–14). Despite this research, some aspects of infection remain elusive including the cellular factors which aid or inhibit HIV-1 (8, 15, 16).

Once HIV-1 infects a cell, multiple cytokines and chemokines are released leading to activation of the immune system (10, 17, 18). Constant activation leads to inflammation and adverse effects (17, 18). For example, dementia-associated symptoms can develop in patients despite having HIV-1 controlled by cART (13). Patients on cART have low levels of viral production less than 50 viral copies per milliliter (19). This low level of production causes constant inflammation due to chronic immune activation (13, 19). When inflammation occurs in the central nervous system (CNS) varying severities of dementia can manifest, called HIV-1-associated dementia (HAD), HIV-1-associated neurocognitive disorder (HAND) and finally

HIV-1 encephalitis (HIVE; (13)). Microglial cells and astrocytes are the cells responsible for causing inflammation in the CNS (20, 21). Microglial cells are responsible for the clearance of cellular debris and phagocytosis of pathogens, and astrocytes make the framework of the brain and form the blood brain barrier (BBB; (21, 22)). The BBB is a highly selective membrane, which inhibits therapeutic drug translocation into the CNS (21). This inhibits therapeutic agents from acting on infected cells and leads to the formation of viral reservoirs in the CNS and the neurological symptoms of HAD/HAND (21). Microglial cells responses to infection and host factors involvement with infection are areas of research with the possibilities of finding other therapeutic interventions which can reduce HIV-1 replication in the CNS (23). Effective therapeutic agents are needed to help with HIV-1 strains that are resistant to some antiretroviral drugs. By investigating the role host factors play in HIV-1 infection, knowledge can be obtained about how host factors play a role in infection and the identification of a possible therapeutic target which reduces HAND/HAD (8, 13, 24). Host factors can be utilized in combination with other therapeutic agents to aid in stemming the small amount of HIV-1 production in the CNS.

Inflammation and Infected Cell Types

To cause disease, HIV-1 infects specific cell types including; CD4⁺ T cells, macrophages, dendritic cells (DC), microglial cells, and astrocytes (8, 11, 18, 25–27). CD4⁺ T cells are the primary target of HIV-1 and must become activated for infection to ensue (11). The first cell types infected however, are macrophages and dendritic cells (11). These cells migrate in the vasculature and various tissue parenchyma of the body to include: the lungs, gastrointestinal tract (GI) and below the epithelial layer (Figure 1;(11)). The main activity of macrophages is phagocytosis of pathogens and cellular debris. Macrophages are also responsible for

transportation and presentation of pathogen antigens or pathogen-associated molecular patterns (PAMPs) to CD4⁺ T cells (11). When tissue damage occurs, living cells signal that damage needs to be corrected (28–30). In the situation where pathogens are identified, the cell will signal an event to clear the infection. This signal is known as inflammation and is constituted by numerous agents (26, 31–35). The signaling agents responsible for inducing inflammation and other immunological functions include chemokines and cytokines (30, 36). Various chemokines and cytokines are released from cells depending upon the stimuli (30, 32, 37, 38). When any infectious event occurs, pathogenic protein binds to pathogen recognition receptors (PRR) which include toll-like receptors (TLR; (39)). Once bound, TLR propagates a signal pathway which releases interleukins, chemokines and interferons that are targeted for the type of infection, for this case HIV-1 infection. There are a total ten TLR, with TLR 3, 7, 9 responding to viral and other foreign genetic material (28, 40).

Once TLR 3, 7, 9 are bound with viral or foreign DNA, IL-22, IL-6, IL-15, IL-8, IL-21, IL-10, interferon (INF) and IL-1 β are released (14, 30, 32, 33, 38, 41). The dispersion of interleukins and other immune signals cause physiological properties to transpire which include; dilation of blood vessels, macrophage extravasation from the vasculature to the tissue parenchyma, and activation of the immune system (17, 36, 40, 42–44). Once in the parenchyma, macrophages eliminate cellular debris, clear infection, and stimulate repair. If HIV-1 virions are within material that invades the parenchyma tissue it is one-way HIV-1 constitutes infection (11). Once infected, macrophage do not succumb to HIV-1, but instead migrate out of the parenchyma and transgress to a lymph node which is an area where CD4⁺ T cells and other immune cells conjugate (11, 43). Macrophage migration to a lymph node is thought to disseminate HIV-1 by activating CD4⁺ T cells and infecting them with HIV-1 (11, 43).

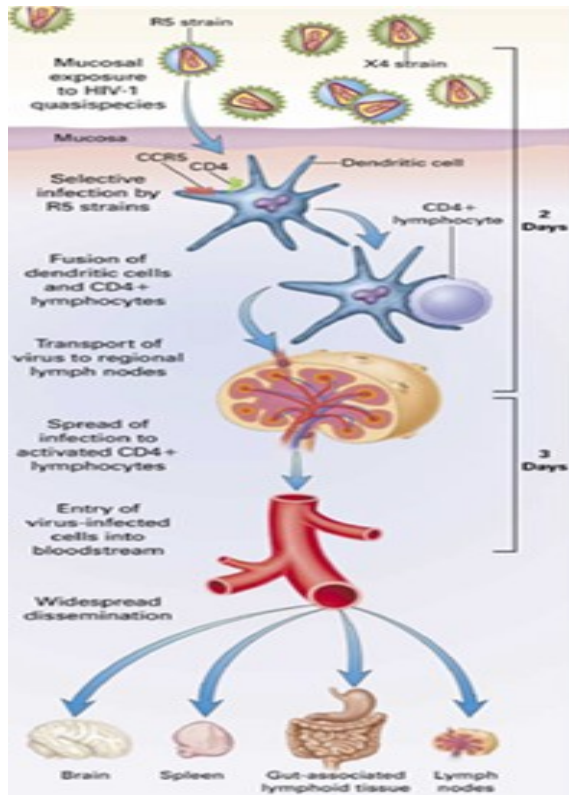


Figure 1. Schematic of HIV-1 Dissemination Throughout the Body. The diagram shows how HIV-1 crosses the various mucosal and epithelial layers to infect immune cells in the tissue parenchyma. One of the first immune cells to become infected are macrophages and dendritic cells which will migrate throughout the body once infected. This is one theory in which HIV- 1 spreads to multiple organ systems in a rapid succession. Once macrophages reach the CNS, HIV- 1 crosses the BBB, infects the resident microglial cells and astrocytes. The infection of resident cells of the CNS causes a viral reservoir to form which leads to HAD/HAND (45).

Infected macrophages not only phagocytose pathogens but also release cytokines and chemokines associated with an immune response (21). Within the confines of a lymph node, cytokines released activate CD4⁺ T cells. Once activated, CD4⁺ T cells produce cytokines associated with the pathogen and activate the adaptive immune system (25, 46, 47). This is a complicated process that involves activation of B cells, natural killer cells and CD8⁺ T cells. Most patients experience flu-like symptoms during this acute phase of infection. One of the cytokines that is involved with orchestrating an immune response is IL-27 (8, 24, 42, 48). IL-27 is an anti-inflammatory cytokine that is part of the IL-12 family of cytokines (49). The IL-12

interleukin family is made up of combinations of α and β -chains with IL-27 containing a p28 subunit along with an Epstein Barr-induced gene 3 (49). IL-27 has been shown to have inhibitory effects with HIV-1 infection in a variety of cells (8, 15, 16, 27, 49). The effects of IL-27 can be seen by the activation of the Jak/STAT pathway and MAP53 intermediate (27, 42, 48). IL-27 along with many other interleukins interacts with a variety of immune cells and creates a systemic fight against HIV-1. Along with $CD4^+$ T cells becoming activated they are also infected with HIV-1 (25, 50). HIV-1 infects T cells and is disseminated throughout the body when afflicted macrophages present viral antigen to activate adaptive immunity. As the macrophages travel to various parts of the body to present antigen to T cells, HIV-1 is being produced and is one way in which HIV-1 is dispersed though out the body. Once infected, $CD4^+$ T cells perish to the virus and decrease in number (11). The decrease in $CD4^+$ T cells, below 200 cells per milliliter, makes it difficult to fight off opportunistic infection and leads to the development of AIDS (1). Not only do macrophages travel to lymph nodes but to the CNS as well via the vascular system (51, 52). However, macrophages do not readily cross the BBB, but due to the systemic response which forms from activation of the adaptive immune system the BBB degrades slightly allowing macrophages to penetrate the CNS (43).

The BBB is a highly selective structure in the CNS to defend against toxins and other pathological agents (53, 54). Astrocytes in the CNS makeup the framework which holds the CNS together, forms the BBB and nourishes neurons (54). Astrocytes form the BBB when projections stem from the cell wrap around neurons and the capillary network feeding the CNS (54). This formation allows astrocytes to support neurons and allows in only essential elements that support neuronal cells (54). However, due to the systemic response caused by $CD4^+$ T cells production of cytokines, the BBB around the vasculature degrades (53). HIV-1 infected macrophages

migrating in the vasculature then pass the BBB and enter the CNS (51). While in the CNS, HIV-1 virions bud off infected macrophages and infect microglial cells and astrocytes in the CNS. Therapeutic agents like cART cannot readily cross the BBB, preventing them from slowing viral replication and leading to the eventual degradation of neurons. This facilitates the formation of a viral reservoir and leads to symptoms of HAD/HAND (11).

Microglial cells are a subset of macrophages and are in the CNS (55, 56). Both cell types possess similar immune receptors, carry out the same physiologic function, are relatively long-lived cells and resist HIV-1 (56, 57). Once infected, microglial cells cause inflammation by further increasing cytokines and chemokines concentration (58). Due to microglial cell resistant nature to HIV and longevity of the cell, it facilitates the establishment of a viral reservoir (21, 22). As astrocytes and microglial cells become infected, they are a constant source of inflammation. When astrocytes become infected it leads to immune activation and causes the breakdown of the BBB (54). When astrocytes die, they can no longer nourish neurons and eventually the neuron itself dies (54). The death of neurons in the CNS causes neurological symptoms seen in HAD/HAND. Therapies are needed to reduce the amount of viral production in microglial cells and astrocytes, which reduces inflammation and neurological symptoms.

HIV-1 Virus, Proteins and Replication Cycle

HIV-1 is a lentivirus and part of the *Retroviridea* family (1). There are two HIV viruses, each with multiple strains and subtypes (59, 60). The first species of HIV is HIV-1 and is related to Simian Immunodeficiency Virus (SIV) in chimpanzees (59). The second type of HIV is HIV-2 and has many commonalities to SIV, however, it has origins in sooty mangabeys (60). HIV-1 has undergone much genetic mutation, which has led to the development of many subtypes (3, 59).

HIV-1 M strain is the epidemic form, and the subtypes include A, B, C, D, F, G, H, J, and K (3). Fifty-one circulating recombinant strains (CRF) exist, and patients have been infected with two or more separate HIV strains (3). HIV strains recombine genetic material and can make new viral strains with higher propensity for progress into AIDS (3).

HIV-1 is an enveloped virus containing two copies of single stranded RNA genome (Figure 2). The HIV-1 genome is 9.7 kb in length, encompassing three polyproteins and multiple accessory proteins (Figure 3;(61)). The polyproteins require multiple rounds of processing by host and viral proteases to activate 9 proteins with specific function (1). The Gag polyprotein contains structural proteins one of which is the capsid (CA; (1)). Gag is cleaved by the viral encoded protease enzyme (PR) to yield three separate functional proteins: matrix protein (MA) or p17, capsid protein or p24, and nucleocapsid (NC) or p7 (7). The matrix protein is located on the inside of the HIV-1 virion and has been implicated in viral assembly and nuclear import (27). The nucleocapsid is a protein that will surround the genomic material and is involved in the reverse transcription processes (28). The capsid monomers will arrange in an organized pattern to create the capsid core (29, 30). The capsid core is a conical, or bullet shaped structure that consists of 1000-1500 capsid monomers which form 250 hexamers and 12 pentamers (29, 30). The Env polyprotein contains proteins associated with the envelope of HIV-1 (1). Env is cleaved by host proteases at the host membrane to yield gp120 and gp41 (7). Gp41 is a transmembrane protein and gp120 is the protein that interacts with the receptor and co-receptor located on the host cell surface (7). Finally, Pol polyprotein encodes enzymatic proteins (1). Pol undergoes a subsequent cleavage to three proteins: reverse transcriptase (RT), integrase (IN) and the protease itself (7). The genomic structure can differ between HIV-1 and HIV-2 viral species. HIV-2 will contain Vpx, an accessory protein that will not be discussed due to the focus on HIV-1 (1).

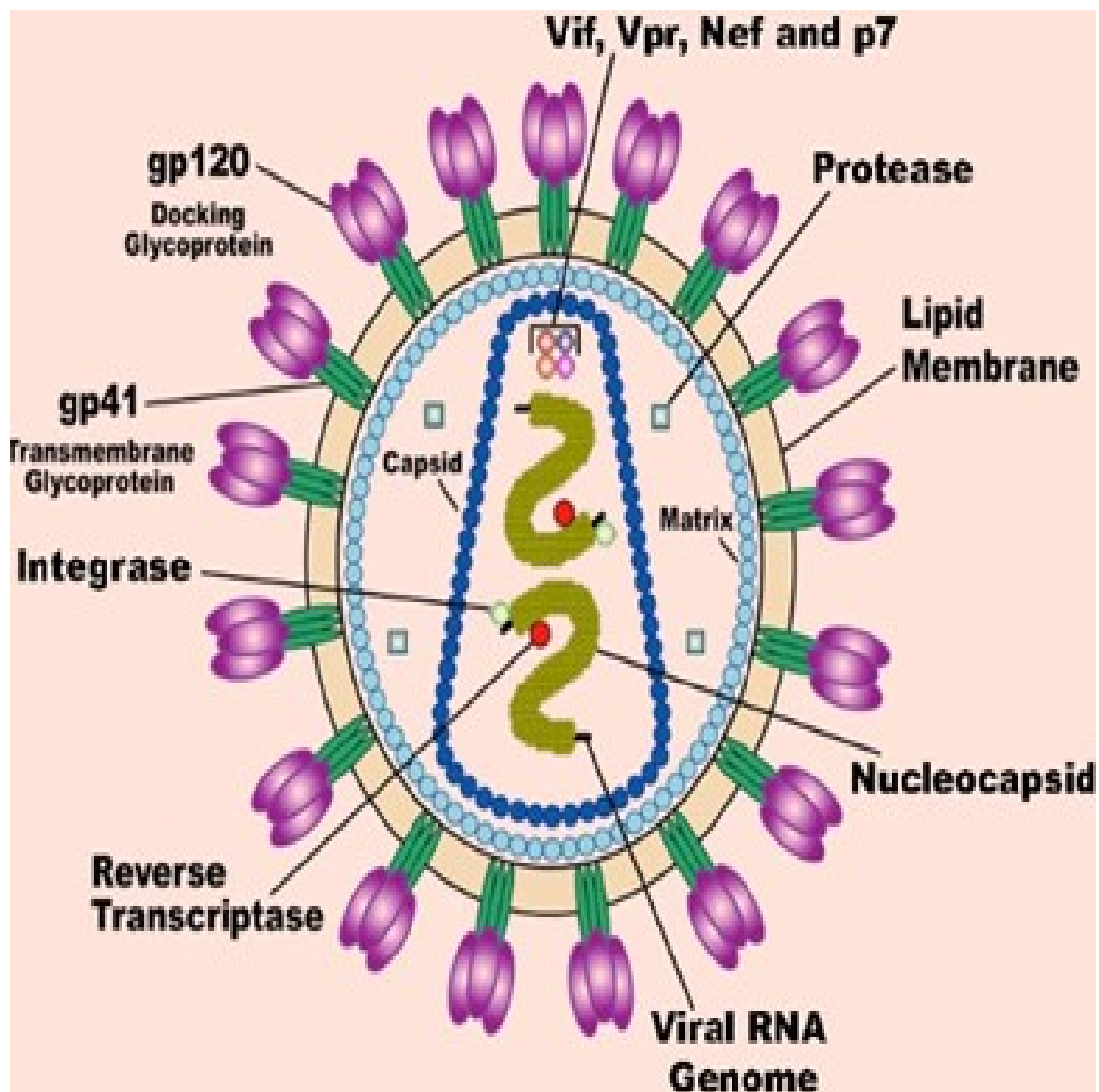


Figure 2. Diagram of the HIV-1 Virion and Protein Location. The graphic representation shows a HIV-1 virion with the location of the structural and accessory proteins. The structural proteins include gp120, gp41 integrase, capsid, nucleocapsid, protease, reverse transcriptase, and matrix protein. These proteins are directly involved in various processes that HIV-1 undergoes to infect permissive cells. The accessory proteins include Vif, Vpr, Nef and others. These proteins' roles include assisting with viral processes, which include dampening the immune response and alteration of host proteins to assist with the infection process. (62)

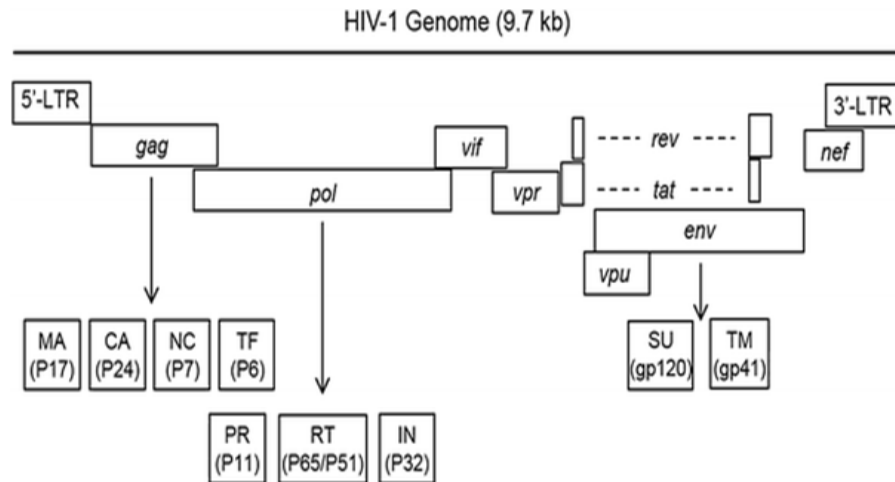


Figure 3. Schematic of the Viral RNA Genome of HIV-1. The diagram shows the viral RNA genome of HIV to include: the length in kilo base pairs, order of the polyproteins and the proteins that reside in them. The schematic also depicts the location of accessory within the RNA strand. The image also shows the name of each of the proteins and other viral proteins that HIV contains. The figure also shows the 5' and 3' LTR. (63)

Polyproteins and their functional proteins are required for HIV-1 infection. However, these proteins are still not enough to cause efficient HIV-1 infection. HIV-1 contains accessory proteins or virulence factors, which increase infectivity by assisting with evading the immune system, down regulation of host proteins, shuttling of proteins from the nucleus to the cytoplasm, and regulation of viral protein production. Virulence factor or accessory proteins include viral protein R (Vpr), viral protein U (Vpu), negative regulatory factor (Nef), regulator of expression of virion protein (Rev), trans-activator of transcription (Tat) and finally, viral infectivity factor (Vif;(1, 64)). Vpr has been suspected in inactivating multiple host factors including UNG2, Dicer, IR3, ZIP, APOBEC3G and others (64). Thus, Vpr prevents an immune response to HIV-1 allowing the virus to escape from host immunity and facilitating infection (64). Vpu has similarities to Vpr in that Vpu down regulates host immunity and increases the infectivity of HIV-1, by modulating host protein BST-2 which is an effector of the innate immune system (65). Nef will down regulate CD4 cellular receptors which will help the viral progeny bud from the

cells (66). This virulence factor will also prevent the cell from mounting an appropriate immune response by down regulating the immune receptor Human Leukocyte antigen (HLA; (66)). Rev is a critical factor in transportation of viral RNAs (67). RNA associated with HIV-1 is transcribed in the nucleus and transported to the cytosol by Rev (67). Transcripts are subsequently translated into viral proteins which associate with genomic material and assemble into virions that bud off the cell. Thus, Rev increases infectivity of HIV-1 by regulating the amount of RNA transported to the cytosol (67). Tat is responsible for increasing the amount of transcript produced from the integrated DNA of HIV-1 by activating RNA polymerase II (68). The last accessory protein, Vif, is used by HIV-1 to inactivate host factor APOBEC3H by targeting this protein for degradation (69). If Vif is missing from HIV-1, infection can still occur, but the extent of infection is greatly decreased.

For HIV-1 to infect cells, a highly ordered and timed replication cycle occurs (Figure 4). This replication cycle can be divided into early and late stages (1, 70). The early stages include entry into a permissive cell, reverse transcription, uncoating, migration to the nucleus, nuclear import, and integration of viral genetic material with the host genome (1). The late stages of HIV-1 infection consist of production of viral protein and genetic material, virion assembly, budding off the cell and maturation of HIV-1 virions (1). The outcome of the early stages is to ultimately enter the cell and integrate with the host genome which establishes infection. The result of the late-stage processes is to produce mature virions which spread HIV-1 to other cells or individuals. Within each stage of the replication cycle significant events occur which facilitate infection. During the replication cycle viral proteins, accessory factors and host proteins play diverse roles which can either inhibit or aid infection (1, 9, 38, 70, 71).

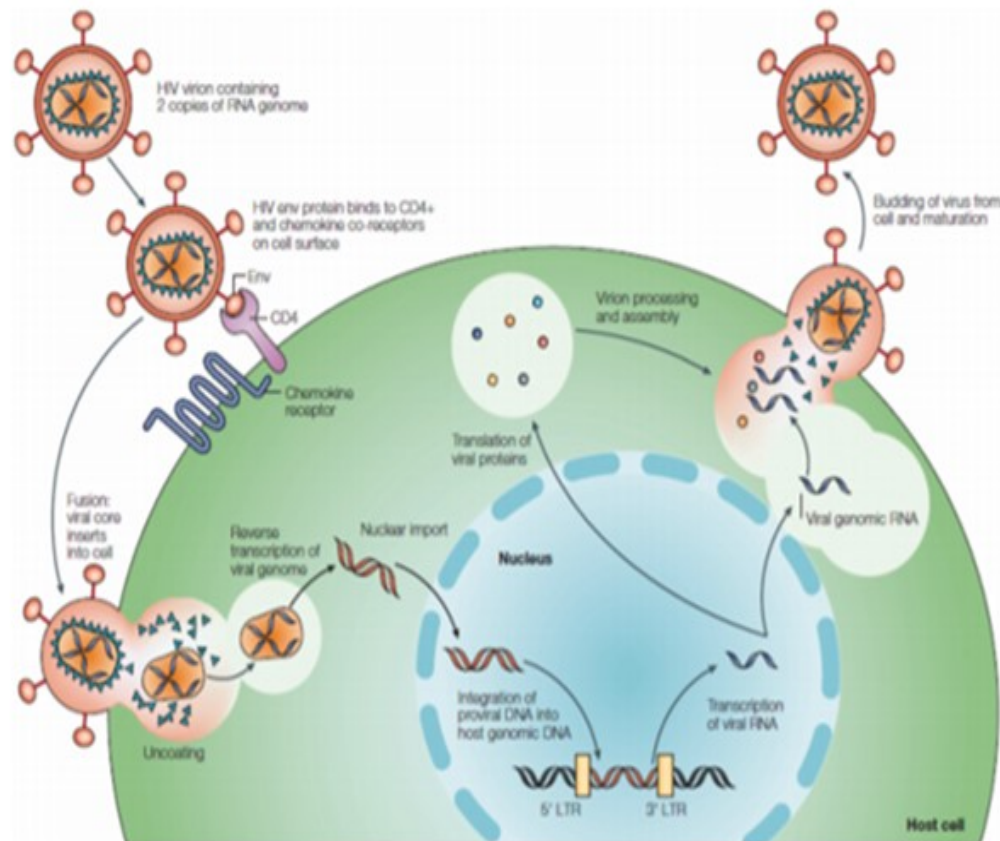


Figure 4. HIV-1 Replication Cycle. This figure shows the replicative cycle of HIV-1. The cycle initiates with binding of the receptor and co-receptors. Subsequent replicative steps include fusion of the host and viral membranes followed by uncoating of the capsid core. As the capsid core degrades it travels to the nucleus of the cells and forms the RTC which facilitates reverse transcription. Once HIV-1 reaches the nucleus the capsid core fully uncoats and forms the preinitiation complex. The PIC facilitates nuclear import of viral DNA into the nucleus. Once in the nucleus proviral DNA is integrated into the host genome via integrase. Transcription ensues followed by translation of viral proteins and DNA. Viral RNA and protein assemble, bud off the cell and mature, completing the replicative cycle. (72)

Binding, Fusion, Uncoating and Reverse Transcription of HIV-1

The initial step in the replication cycle occurs when HIV-1 binds to the CD4⁺ receptor and CCR5/CXCR4 coreceptors of susceptible cells (1, 61). From here the CD4⁺ receptor will be referred to as receptor and the CCR5/CXCR4 will be referred to as the co-receptor (1, 61). Binding initiates when gp120, which is integrated on the viral membrane, binds with the receptor and co-receptor (1, 61). Following binding of the receptor/coreceptor, fusion of HIV-1 ensues,

and the viral and cellular membrane combine via a conformational change in gp41 (1, 61). The conformational change occurs when gp120 binds to the receptor/coreceptor and induces a change in gp41 to a 6-helical bundle structure (73). The creation of the 6-helical structure exposes the fusion-promoting peptide and initiates the combination of the two membranes (74). After the union of the two membranes the capsid core is released into the cytoplasm and uncoating along with migration to the nucleus ensues (61). Once HIV-1 binds to and starts to fuse with the cell it will encounter one of the first cellular components that can aid or inhibit infection, the cortical actin cytoskeleton (75, 76). Binding of HIV-1 to the receptor/coreceptor propagates a signal transduction pathway which leads to increased receptor stability and clustering (74). The clustering of the receptor and coreceptor leads to an increase in Env, the receptor and coreceptor interaction which promotes fusion of the two membranes (74). There are some reports that viral proteins can interact with cortical actin or hijack other proteins to alter cortical actin (74, 75, 77).

The other entry method that HIV-1 can take to enter the cell is by endocytosis (75). This method is commonly utilized in research to infect cells not normally permissible to HIV-1 infection. This is accomplished by changing the envelope of HIV-1 to the vesicular stomatitis virus VSV-g envelope (VSV-g). The change in envelope allows HIV-1 virus to enter the cells via endocytosis rather than fusion of the host and viral membranes (75). The endocytic method is mediated by clathrin, and HIV-1 is taken up into endocytic vesicles (75). Once HIV-1 is in the endosome the virus eventually fuses in a coordinated process that will release the capsid core into the cytoplasm. This is one way in which HIV-1 can bypass the physical barrier of the cortical actin cytoskeleton at the membrane.

Once the capsid core is in the cytoplasm the virion migrates to the nucleus via microtubules or the actin cytoskeleton (9, 71). The capsid core will eventually degrade or

disassemble in a process called uncoating (78). The average capsid has a length of 119 nm and a width of 61 nm (79). The capsid core is made up of 1000-1500 capsid monomers which arrange into 250 hexamers and 12 pentamers. The pentameric structures of the capsid core are located at the angles or curvatures and hexamers compose the rest of the capsid structure (78). The configuration of pentamers and hexamers allows for the bullet or conical morphology of the capsid core (Figure 5). Hexamers, along with pentamers are organized by adherence of multiple capsid monomers in a circular fashion at the Carboxy-terminal domain [CTD; (80)]. This forms a CTD-CTD junction and holds the structures together (80). The N-terminal domain (NTD) of pentamers/hexamers are located on the exterior aspect and facilitate linkage of multiple units (80). The joining of pentamers/hexamers form the capsid core allows structure stability and protects the genetic material of HIV-1. Since each individual capsid core has a varying number of monomers, the stability of the capsid core is different from virion to virion (81). This varying stability alters uncoating kinetics of HIV-1 and adds to the unknowns of the uncoating process.

As the capsid core migrates to the nucleus the genomic RNA will be reverse transcribed into DNA in a process called reverse transcription (39). When hexamers/pentamers form they arrange in such a way that a small hole is created in the center of the structure (82). The centralized hole is called the IP6 hole and is composed of hydrophilic amino acids (82). The hole exists in two conformations, open and closed, which allows dNTPs into the capsid core (82). In the open confirmation dNTPs enter the capsid core and are incorporated into the newly synthesized strand of viral DNA (82).

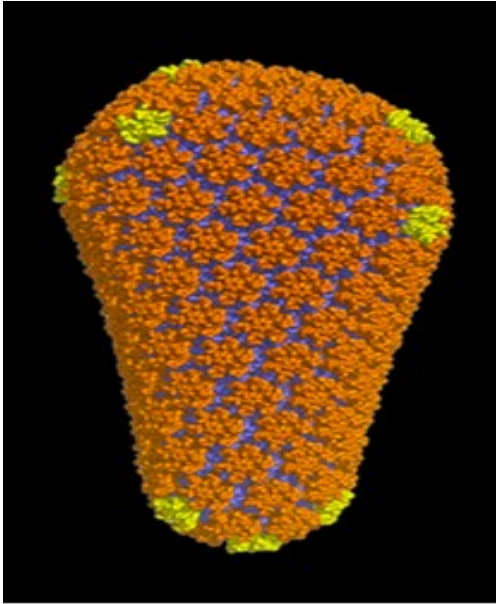


Figure 5. Capsid Core. This image details the capsid structure, the hexamers are in orange and the pentamers are in yellow. Both of which are made from monomers and held together by the CTD-CTD junction. In the middle of the hexamers, you can see the hole which allows dNTP into the core. It is held together at the NTD-NTD junction between each of the individual units (5).

As viral RNA is transcribed into DNA, the triggering event is initiated which causes uncoating to begin (83). One proposed trigger that commences uncoating is strand transfer, in which the first 137 bp of the first 5'LTR is reverse transcribed and that strand of ssDNA will then be transferred to the second strand which helps facilitate reverse transcription in the second RNA strand (Figure 6;(83)). Other evidence notes that as viral RNA is reverse transcribed into DNA it causes a buildup of pressure (84). The increase in genomic material causes pressure to increase which puts stress on the capsid core (84). This increased stress causes the pentamer/hexamers to break away from the capsid core (84). Thus, the increased pressure from the accumulation of genetic material assists or causes the capsid core to fall apart (84). Both reverse transcription and uncoating are integrated with one another, in that if one process is altered then the other process is affected as well (80, 83, 84).

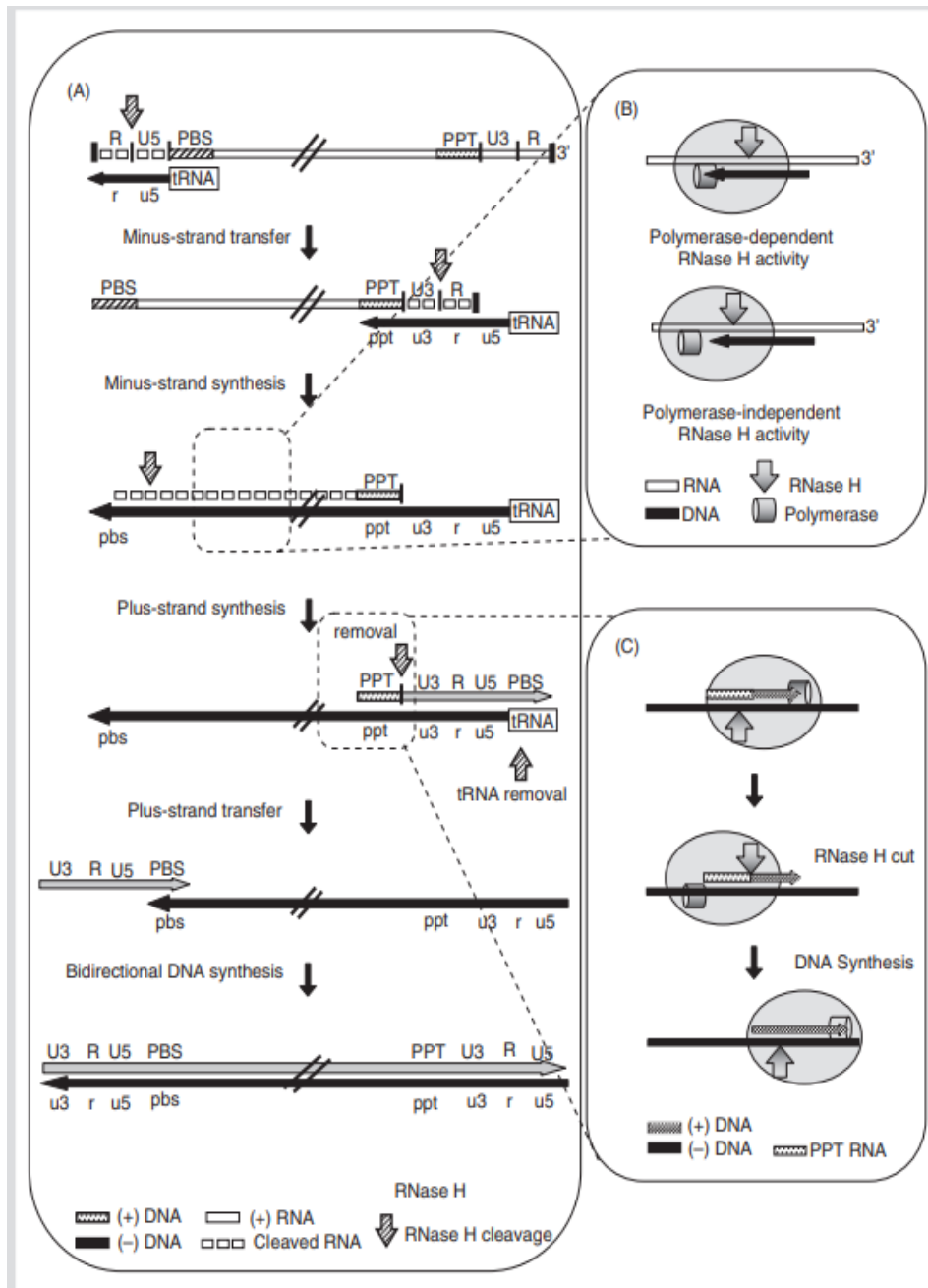


Figure 6. The Strand Transfer of HIV-1. This diagram shows how the first 137 bp of one of the RNA stands of HIV is reverse transcribed into DNA. The small fragment of DNA will transfer to the other strand of RNA and initiate the change to DNA. It is this transfer that is thought to initiate the uncoating process. Another avenue that could play a part in uncoating is the buildup of genomic material. Since this process occurs in the confines of the capsid core the accumulation of products can cause stress on the capsid core and cause it to disassemble and break apart. (85)

Three separate models exist to describe when uncoating and reverse transcription takes place (Figure 7;(5)). The first model called immediate uncoating proposes that the capsid core degrades immediately after fusion (5). After the capsid core degrades, reverse transcription occurs and genomic material transverse the cell which ultimately integrates with the host genome (5). However, the immediate uncoating model has recently been discredited and research points to the other two proposed models. In the second proposed model of uncoating, called biphasic uncoating, the capsid core is released into the cytosol and transgresses to the nucleus (5). Figure 7 shows that during the migration, reverse transcription occurs inside the capsid core (5). After some relatively unknown initiating event, uncoating of the capsid occurs slowly by the dissociation of the capsid hexamers/pentamers (5). In the biphasic model the full degradation of the capsid core is completed close to the nuclear envelope (5). Full degradation of the capsid core allows the genetic material to undergo nuclear import and integrate into the host genome (5). The biphasic model also allows for some of the capsid hexamers and pentamers to remain in proximity to the nucleus to facilitate nuclear import (5). The last model of uncoating called NPC uncoating demonstrates that the capsid core remains intact until it reaches the nuclear envelope (5). Once the capsid core reaches the nucleus the core degrades, and viral DNA enters the nucleus (5). During this model reverse transcription occurs in the confines of the capsid core and allows for the capsid protein to aid in nuclear import (5).

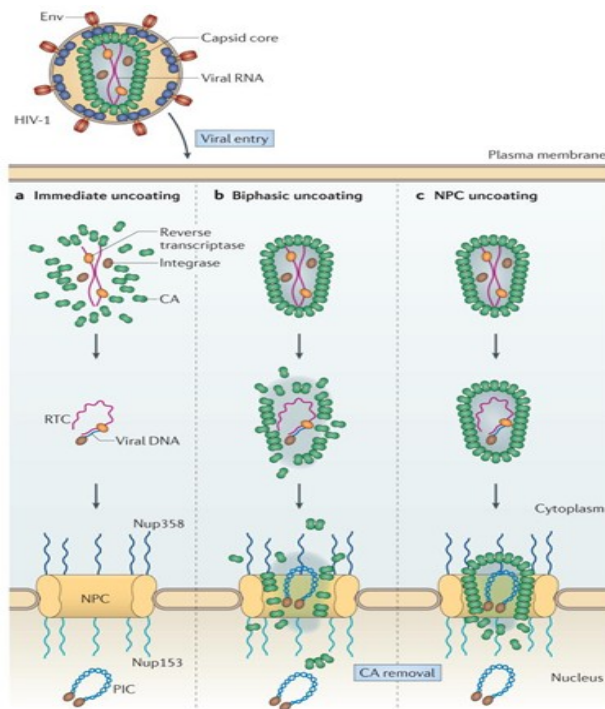


Figure 7. Models of Uncoating. This depiction shows the three models of uncoating. The first model of uncoating is called the immediate uncoating, it shows the capsid core immediately degrading upon entry into the cell. Reverse transcription then occurs, the RTC then migrates to the nucleus, undergoes nuclear import, and inserts with the host genome (A). The biphasic model of uncoating shows the capsid core being released into the cytoplasm upon entry into the cell. The capsid core starts to migrate to the nucleus and reverse transcription occurs. During migration, the core will start to degrade due to an unknown trigger. Once the core reaches the nucleus it will fully degrade and undergo nuclear import and inserts into the host genome (B). In the NPC model of uncoating the capsid core stays intact for the entire migration to the nucleus and RT proceeds in the core. Once the core reaches the nucleus the core will degrade, and the genetic material will undergo nuclear import and insert into the host genome (C; (5)).

Nuclear Import, Integration and Production of Progeny Virions

Following uncoating and reverse transcription, the preinitiation complex (PIC) assembles which allows the genomic material to undergo nuclear import (80). The intact capsid core cannot cross the nuclear envelope due to size restrictions and must degrade for nuclear import of viral DNA (5). Capsid monomers being found inside the nucleus of an infected cell suggest that the capsid protein it participates in nuclear import (86). Host nuclear envelope proteins NUP153 and NUP 358 are located on the nuclear pore and are thought to bind to capsid monomers and

facilitate entry into the nucleus (5). After HIV-1 has undergone nuclear import, integrase inserts the cDNA of HIV-1 into the host cell genome.

In the later steps of HIV-1 replication, host replication machinery will transcribe the newly inserted HIV-1 DNA (1). Viral RNA produced leaves the nucleus by the regulation of Rev and is subsequently translated into proteins. Viral proteins which ultimately came from the insert genetic material of HIV-1 are packaged into virions along with viral RNA which then buds from the cell membrane and completes the replication cycle of HIV-1 (1).

SPTBN1 Structure and Function as a Host Factor For HIV-1

One cellular protein that has been shown to be associated with HIV-1 infection is spectrin beta non-erythrocytic 1 (SPTBN1). SPTBN1 is a host protein that associates with the actin cytoskeleton and acts as a scaffolding protein for actin filaments. This scaffolding allows actin filaments to be held together and form organized units for various functions throughout the cell (87–91). Three studies demonstrated that SPTBN1 is needed for HIV-1 infectivity in various cell lines (8, 15, 16). However, the studies implicate SPTBN1 facilitating different replicative steps from fusion, uncoating and possible migration of the capsid core to the nuclear envelope (8, 15, 16). In the first study, Brass and colleagues performed a siRNA screen on Jurkat cells (CD4+) to investigate cytoskeletal host factors that are associated with wild type HIV-1 (16). Brass identified SPTBN1 as a host factor that facilitates HIV-1 infectivity as there was a decrease in the infectivity when this protein was downregulated. The role for SPTBN1 was not directly assessed in the study but the authors noted that the host factor could assist with fusion, uncoating, reverse transcription and viral trafficking of HIV-1 (16). The second study was performed by Gallo and colleagues, which looked at the role of SPTBN1 in HIV-1 infection in

HeLa cells (15). Researchers knocked down the expression of SPTBN1 along with ten other cytoskeletal proteins using siRNAs and subsequently infected the cells with wild type HIV-1 and VSV-G HIV-1 virus (15). VSV-g HIV-1 is the virus type used for this thesis. VSV-G HIV-1 virus is a pseudotyped virus that enters the cell via endocytosis. When endocytosis occurs, VSV-g HIV-1 fuses with the endosomal membrane rather than the cellular membrane, which is what is seen with wild type HIV-1. This virus also has a mutation in Env which disables the virus from forming properly. This allows VSV-G HIV-1 to only undergo a single round of infection and therefore a safer form of HIV-1 for use in research. Knockdown of SPTBN1 decreased infectivity by 20% when cells were infected with VSV-G HIV-1, whereas knockdown of SPTBN1 in cells infected with wild type HIV-1 decreased the infectivity more than 40 % (15). This suggested that the entry method of the virus plays a role in the infectivity and that SPTBN1 plays a role in fusion of HIV-1. There was no further investigation of the role of SPTBN1 in this paper. These two papers showed that the downregulation of SPTBN1 decreases HIV-1 infectivity with mounting evidence denoting its role in the fusion process. However, there remains a gap in knowledge in how or if SPTBN1 participates in fusion of HIV-1. This needs to be investigated to understand how host factors participate in various processes of HIV-1 and this is the third aim of my thesis.

Dai and colleagues found that when monocytes are differentiated into macrophages by IL-27, SPTBN1 was downregulated (8). The down regulation of SPTBN1 corresponded to a decrease in HIV-1 infectivity. Researchers differentiated monocytes into macrophages with M-CSF (M-mac) or IL-27 (I-mac) and then infected with wild type HIV-1 (8). Following infection, the amount of HIV-1 infection was determined by tabulating the production of capsid protein produced in cell supernatant (8). I-mac cells showed a drastic decrease in the amount of capsid

protein produced over a 24-day period post infection when compared to the M-mac cells (8). When the two cell lines were infected with VSV-g GFP HIV-1, infectivity was analyzed by fluorescence assisted cytometry (FACS). FACS is a type of cytometry which utilizes a fluorescent label to denote an infected cell, specific protein expression, or other cell properties. When the labeled cells are placed in the flow cytometry the instrument can count and separate the cells based on the fluorescent label. From the number of cells that express a fluorescent label, information can be determined to include, the percent of cells that are infected, receptors expressed on the cells, and other aspects of the cells. The I-mac cells showed a decrease in infectivity of about 80% when compared to the M-mac cells.

The Dai study noted the different differentiation processes (CSF or IL-27) did not alter the physiological processes of the macrophages. Both I-mac and M-mac cells showed the same migration response/distance to chemotactic agents SDF-1 α or RANTES (8). The same trend was seen in the phagocytic ability when no difference was seen in the response to *E. Coli* (8). FACS showed the same receptors for differentiation at the same level between I-mac and M-mac cells (8). Finally, the immune response was tested by the Milliplex assay kit which tests the production of cytokines and other immune markers produced by the cell and showed no difference between the two cells (8). Researchers noted that both cell lines expressed the same amount of receptor and coreceptor which suggest that binding of HIV-1 is unaffected.

Dai conducted genome-wide gene expression analysis and found 178 genes were differentially expressed between the two cell lines, with 60 genes having decreased expression and 118 genes with increased expression. From here, heterokaryons were made by fluorescently labeling the cells and combining the two cell types. The I-mac cells were labeled red, and the M-mac were labeled green. Heterokaryons, which were a combination of I-mac and M-mac,

appeared yellow. The heterokaryons were infected with VSV-g HIV-1 and showed an increase in HIV-1 infection when compared to homokaryons of I-mac cells. The results from the heterokaryon experiments pointed to a missing host factor in the I-mac cells that was essential for HIV-1 infection. Sixty downregulated candidate genes in the I-mac cells were cross referenced with 11 previously identified host factors. SPTBN1 was present on both groups. A Western blot and qPCR confirmed the decrease in SPTBN1 expression levels in the I-mac cells (8). To confirm SPTBN1 played a role in HIV-1 infection, researchers were able to rescue infection in I-mac cells by inserting a vector that contained SPTBN1 into I-mac cells (8).

To determine how SPTBN1 was facilitating HIV-1 infection, researchers looked for a direct interaction between SPTBN1 and different HIV-1 proteins. Immunoprecipitation assays showed that SPTBN1 could bind to Gag. However, more importantly SPTBN1 bound the capsid protein and nucleocapsid protein of HIV-1. To confirm the interaction of SPTBN1 with Gag researchers fluorescently labeled the two proteins (8). When the fluorescent images of SPTBN1 and Gag were merged the R value was calculated to be 0.724 which indicated the colocalization of the two proteins. To demonstrate the interaction between HIV-1 and SPTBN1, both were labeled with a fluorescent dye. In the M-mac cells 75% of the virions were associated with SPTBN1 and 13% of the virions were associated with SPTBN1 in the I-mac cells. When SPTBN1 was downregulated, I-mac cells showed an alteration in the architecture of the actin cytoskeleton in which more than 50% of the F-actin fibers were replaced with granular or punctate actin. This alteration in the actin cytoskeleton related to a drastic decrease in HIV-1 infectivity. The disturbance in the actin cytoskeleton corresponded to a decrease in infectivity with not only HIV-1, but with herpes and influenza viruses as well.

The exact mechanism of SPTBN1 influence on HIV-1 still eludes researchers (8,15,16). However, a role for SPTBN1 in HIV-1 infection is proposed to involve the actin cytoskeleton and various parts of the replication cycle to potentially include fusion, viral trafficking, and uncoating (8,15,16). Some of the research indicates that SPTBN1 assists with uncoating based on the Dai publication showing an interaction with the capsid protein and the nucleocapsid (8). Other possible roles for SPTBN1 in HIV-1 infection include fusion (15,16). This evidence is based in that HIV-1 viruses with different envelope proteins are affected differently by the downregulation of SPTBN1 (15). SPTBN1 seems to play a bigger role in WT HIV-1 infection compared to VSV-g HIV-1 (15). SPTBN1 could also assist with viral trafficking. Since SPTBN1 can associate with the actin cytoskeleton and the capsid protein, it could act as an adapter protein, attaching the capsid core to the actin cytoskeleton to assist in migration through the cytoplasm (8,16). One unlikely area in which SPTBN1 could possibly play a role is in reverse transcription. No evidence has been presented that SPTBN1 plays a role in this replication process. However, due to the close association of uncoating with reverse transcription, this process could be indirectly affected.

It is clear from previous studies that SPTBN1 is cell specific and virus strain dependent (8,15). In the Dai publication IL-27 did not affect the expression level of SPTBN1 in 293T and HeLa cells (8). The same publication showed that in CD4⁺ T-cells and dendritic cells the downregulation of SPTBN1 had no effect on HIV-1 infectivity (8). In macrophages however, SPTBN1 seems to play a bigger role in the infection process than other cell lines (8,15). SPTBN1 knockdown severely depleted HIV-1 infection in macrophages, whereas in its knockdown in HeLa cells, it was only inhibited by 20-40% (8,15). In the Gallo paper, SPTBN1 down regulation affected WT HIV-1 more than the pseudotyped HIV-1.

The discrepancy in the effect of SPTBN1 downregulation in macrophages compared to other cell lines and the differences in VSV-g HIV and WT-HIV infectivity need to be better understood if the mechanism of action for SPTBN1 with HIV-1 can be understood. By understanding how the down regulation of SPTBN1 decreases the infectivity of HIV-1 it could lead to possible therapeutic agent or target. This therapeutic method could reduce cytokine production, inflammation, and the incident of HAD/HAND in patients.

There are two types of spectrin proteins in mammalian cells, erythrocytic and non-erythrocytic (Figure 8). Erythrocytic is known as alpha spectrin or SPTA and is found in erythrocytes (92). SPTA gives structural integrity to erythrocytes to deform and endure high shear stress as it migrates through the vasculature (91, 92). The non-erythrocytic spectrin is found in all other cells and is called beta spectrin or SPTBN (92). Areas of the body which contain the highest amount of beta spectrin are cells of the brain, lungs, and adipose tissue (93). Beta spectrin performs many functions in the body to include interaction with the actin cytoskeletal and cell structure. Both spectrin types can be found at loci NC_000002.12 (54456327..54671446) on chromosome 2 (93). SPTBN1 protein can go by many aliases; ELK, HEL 102, and SPTBNII and β II (93). Spectrin is a protein that is composed of two separate subunits, α 280 kDA and β 247 kDA (92). Each of the subunits of spectrin will have multiple isoforms. The β subunit has 5 isoforms and α has 2 isoforms (93). The various isoforms can recombine which allows for remarkably diverse functionality in the cell (92, 93). Most spectrin proteins are highly associated with the actin cytoskeleton in some fashion (87, 88, 90, 91, 94). This can include binding of the cytoskeleton to the membrane, vesicle trafficking and cytoskeletal scaffolding. The two subunits interact in a head-to-head formation, with multiple residues that allow for various binding sights and cellular function (Figure 8, 92). The fully

formed spectrin protein has a linear length of 37 nm. Spectrin protein can expand and contract from 47 nm to 190 nm based upon physiological properties of the cell including ionic strength, protein concentration, addition, or removal of a section of the plasma membrane, and reduction in temperature (92, 95). Each unit of spectrin is 106 amino acids (AA) long that form into an α -helix structure (Figure 8). The α -helix then folds into a triple helix with linkers that facilitate the turn to another helix (95). The third helix is a partial helix which will interact with one another and finish the triple helix formation in the spectrin tetramer (95). This conformational arrangement allows spectrin tetramers to expand and contract (95). This ability is coined the Chinese finger trap model and allows spectrin to have structural reliance in the cell (95). Each subunit has a repeat section, the α -subunit has a repeat of 20 units and the beta subunit has 16 repeats (Figure 8; (92)).

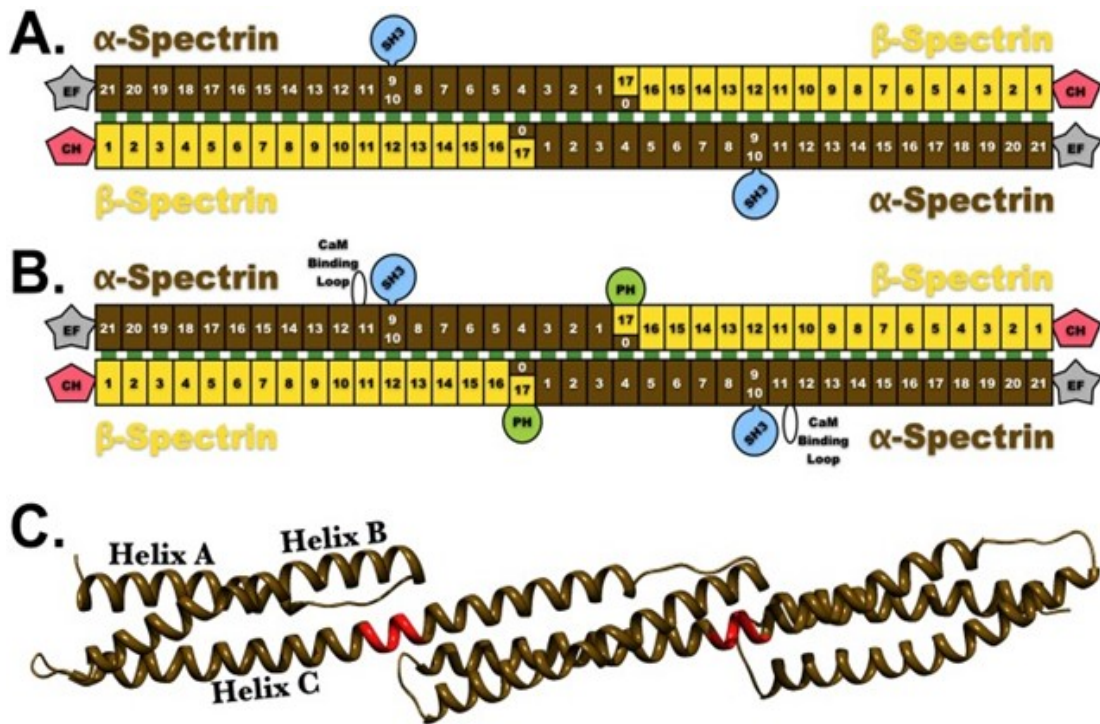


Figure 8. Spectrin Proteins. Two spectrin proteins are found in mammalian cells. Both spectrin types consist of two subunits β and α that are orientated in a head-to-head fashion (A). The schematic shows the erythroid type of spectrin and the various domains. The erythroid type contains a CH domain which binds to actin filaments, the EF domain which binds calcium, involved in signaling protein calmodulin, and can bind troponin-C (B). The schematic shows the non-erythroid type of spectrin this type of spectrin has the same domains as the erythroid with the addition of PH domain which can bind to various other proteins. (C) A ribbon diagram of spectrin. It shows a triple helix structure that shows two complete helices, and half helix that will combine to the other half helix to complex the molecule. The orientation of this protein creates a hole in the middle that can get smaller in diameter as the molecule elongates or constricts. (95)

Different domains and repeats give SPTBN1 the ability to carry out a variety of functions throughout the cell (92). SPTBN1 has a PH domain found near the end of the protein which is involved in binding of specific proteins to facilitate signal transduction, cell proliferation and cellular motility. The beta subunit of SPTBN1 has two CH domains that are associated with the actin cytoskeleton. Other cellular factors that have the capacity to interact with SPTBN1 include phospholipids, PI (4,5), TGF- β , and SMAD3/4 adapter (92). The proteins capable of interacting with SPTBN1 are embedded in the cell membrane and involved in cell signaling and migration. Thus, SPTBN1 acts like an adaptor molecule linking structures in the plasma membrane to the

actin cytoskeleton (92). Other reports state that SPTBN1 is involved in cell to cell contact in that it will anchor E-cadherins to the plasma membrane (94). Another function of SPTBN1 is that it acts like a rung on a ladder and cross links actin filaments together (89). The crosslinking guides the elongating fiber of actin to the plasma membrane (89). In neurons SPTBN1 is involved in the membrane periodic skeleton (MPS) (90). The MPS is made up of F-actin rings that form around the entire length of the neuronal axon (90). Where SPTBN1 comes into play is that it organizes the F-actin rings into uniform spaces apart (90). If SPTBN1 is missing, the spacing is disrupted which causes manifestations of neurocognitive symptoms (90).

SPTBN1 has many functions throughout the cell, with some functions that are critical to cell physiology. In SPTBN1 knock down experiments in mice, the loss of SPTBN1 correlated with a decreased in nerve conductivity and grip strength (89). In a separate publication, authors showed that SPTBN1 is involved in retrograde signaling in neurons (88, 89). There are actin filaments that span the length of the axon which allows for intraneuronal signaling (88, 89). When SPTBN1 was down regulated neurons were unable to send a signal back to the soma of the cell due to disruption of the actin cytoskeleton causing disrupted intraneuronal signaling and neural degradation (87,88). Another vital process that involves SPTBN1 is DNA repair (96). SPTBN1 is involved in stabilization of stalled replication forks (96). This stabilization causes the replication fork to stay open and prevent structural collapse during the repair mechanism (96). Therefore, downregulation of SPTBN1 causes an increase in the amount of replication fork collapse (96). The increase of collapsed replication forks increased the propensity of cancer in hepatocytes in mice (96). Since SPTBN1 is involved with linking F-actin with proteins embedded in the membrane of the cell it can possibly be involved in the Hippo signaling pathway (87). In mammalian cells the pathway is involved with growth control and

tumorigenesis. The authors proposed that it is an upstream regulator of the pathway however, this is not well understood (87). Finally, other reports show that SPTBN1 is involved in trafficking of vesicles. Therefore, the possibility exists that fusion, uncoating and migration to the nucleus of HIV-1 require SPTBN1 interaction with the actin cytoskeleton. This involvement could be why there is a disparity when different virus strains are used in different experimental procedures. If SPTBN1 is going to be used as a therapeutic target for HIV-1, it will have to be targeted in specific cells so that the effect on other activities is reduced and noninfected cells remain unaffected.

The Role of the Cytoskeleton in HIV-1 Infection

The cytoskeleton is an essential structure in the cell that is utilized for various functions from vesicle transport, endocytosis, stability, and cell motility (71, 98, 99). The cytoskeleton consists of three fibers of different sizes; microtubules which are 25nm in diameter, intermediate filaments which are 10nm in diameter and microfilaments (actin filaments) which are 7-9nm in diameter. Microtubules are the largest filament of the cytoskeleton and are composed of α and β tubules. The tubules then assemble in a head to tail fashion which allows the structure to acquire a tube morphology and range from 20 to several hundred nanometers long (71, 100).

Microtubules assemble at microtubule organizational centers (MTOC) which are located throughout cells and have two directional ends which extend to different areas of the cells (100). The positive end is directed to the cell membrane and the negative end is directed to the nucleus of the cell (100). Microtubules have two motor proteins that migrate in opposite directions to facilitate movement of various cargo throughout the cell (71, 101). Dynein, which is directed to the negative end of the tubule, and Kinesin, which is directed to the positive end of the

microtubule. Since microtubules can polymerize with directionality and utilize motor proteins, viruses, including HIV-1, can utilize the structure to carry out various infection processes (12, 71, 101, 102).

Two important infection processes that involve microtubules are viral trafficking and uncoating (71, 101). The two motor proteins are thought to traffic capsid cores to the nucleus and the opposite directionality of the motor proteins is how the viral capsid navigates obstacles that are encountered in the cell (Figure 9; (71)). Dynein and Kinesin are also proposed to assist with disassembly of the capsid core (Figure 9; (101)). The motor proteins pull on the capsid core in opposite directions; increasing the stress and causes the core to disassemble (71). However, the motor proteins associated with microtubules cannot directly bind to the capsid core of HIV-1 and require adaptor proteins to link the two proteins together. FEZ is the adaptor protein that will link Kinesin to the capsid core and BICD2 is the adaptor protein that will link Dynein to the capsid core (102). Other parts of the cytoskeleton play a major role in the infection process of HIV-1 including fusion, uncoating, and transport. Actin filaments or F-actin plays a role in fusion, transport and uncoating. However, HIV-1 components cannot interact with actin filaments. There may be other adaptor proteins like FEZ and BICD2 which associates with F-actin and binds to HIV-1 proteins. This could be how SPTBN1 facilitates infection in that it is able to link the actin cytoskeleton to the HIV-1 proteins.

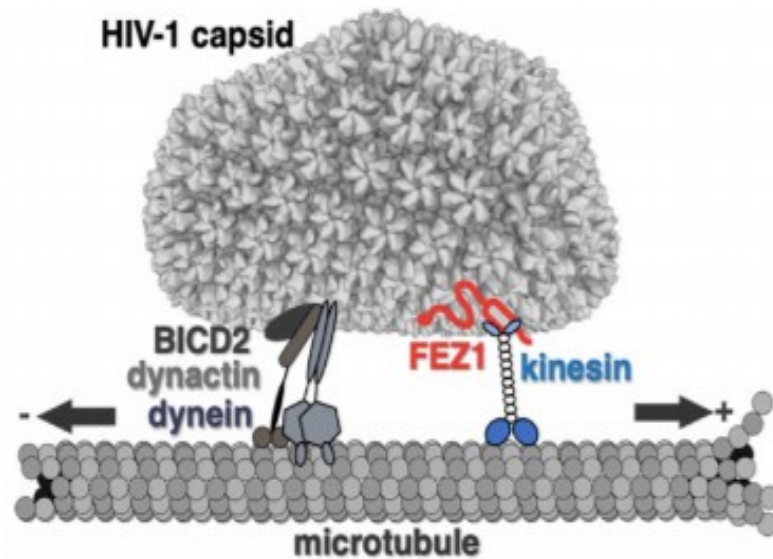


Figure 9. Microtubule Involvement with HIV-1. Adaptor proteins FEZ1 and BICD2 bind to the microtubule motor proteins, allowing the capsid core of HIV to migrate to the nucleus and navigate obstacles. This is also a theory on how the capsid core breaks apart and degrades. Motor proteins attach to the capsid core by adapter protein and move in opposite direction. When the proteins move in opposite direction it will put stress on the capsid core and cause it to degrade (102).

Mammalian cells have two types of actin, globular or G- actin and filamentous actin or F- actin (98). Both G-actin and F-actin can revert between one another to maintain pools of each form within the cells. Each type of actin contains a Mg^{2+} complex with an ATP or ADP binding site to facilitate the change between forms (98, 99). The reversion between forms is orchestrated by ionic strength of various cations. When Mg^{2+} , Na^+ , K^+ are lowered, F-actin transforms into globular actin, the reverse occurs when the ionic strength is increase (97, 98). When G-actin converts to F-actin, the globular orientation reforms to make filaments which consist of fibers which are organized into filamentous bundles (97, 100). F-actin bundles make a double helix in which fiber bundles wrap around one another and repeat every 36 nm (97). Each actin filament contains a positive and a negative ended terminus where other actin filaments will attach (99). The end termini contain binding sites for multiple proteins that facilitate the elongation or

degradation of the actin fibers (9, 74, 98, 99, 103). When cofilin, profilin or the multiunit protein ARP2/3 complex binds actin it will elongate/degrade or sprout branch fibers (9, 104, 105). This allows for diverse functions to include formation of contractile rings during telekinesis, forming the cellular cortex, internal support for microvilli, formation of lamellipodia/filopodia, cell trafficking and phagocytosis (9, 70).

The positive end of the actin filament comprises the ATP binding cleft and is the site of elongation of the actin filament (99). Elongation is initiated by internal/external signals from the cell which cause G-actin to revert to F-actin and elongation of the F-actin filaments. Three phases of elongation proceed and include the nucleation phase, elongation phase, and steady state phase (99). In the nucleation phase, F-actin will combine in two or three subunits which then act as nucleation or starting points for the elongation of actin fibers (97). The elongation phase is based on intracellular concentrations of ATP, below a certain concentration fiber will not elongate. Elongation of actin fibers occurs at both ends but 10 times faster at the positive end than at the negative end (98, 99). When a subunit of F-actin is added, ATP is hydrolyzed to ADP and phosphate group. The F-actin strand will elongate in this fashion until the pool of G-actin is depleted. After the G-actin pool is diminished F-actin will degrade back down into G-actin so that the balance is restored. This equilibrium is the final stage of the elongation process and is termed steady-state-phase. When the ATP is hydrolyzed into ADP it is released from the positive end and travels to the negative end of the filament. The movement and binding of ADP releases a subunit from the negative end of the actin filament. The released subunit then migrates to the positive end of the filament and gets incorporated into the growing strand. The migration of actin filaments from the negative end to the positive end is termed treadmilling and is an efficient way to elongate a strand of actin without depleting the G-actin pool. Other proteins that can cause

actin remodeling is the Arp2/3 complex (9). The Arp2/3 complex is a multiprotein complex that contains 7 subunits and attaches to the actin filament. Once attached the complex Arp2/3 adds actin filaments to the side of the main actin fiber. These actin fibers that protrude from the main filament are called branch filaments. These branches can then be exploited to transport cargo throughout the cell. On its own the Arp2/3 complex is a very weak activator of actin and will need to be associated with nuclear promoting factors (NPF) and other signaling factors for efficient actin remodeling.

Treadmilling is accelerated by the action of profilin, cofilin and capping proteins (Figure 10). Profilin is a protein capable of binding to G-actin. Once bound, profilin rapidly dissociates ADP from the binding sight. The dissociation allows ATP to readily bind the profilin-ATP complex, which is located at the positive end of F-actin. Thus, profilin speeds up binding of subunits to the positive end and extension of actin filaments. Cofilin action in treadmilling is to bind the F-actin subunits and cause a conformational change in the twist of the filament. This change destabilizes actin and causes the negative end of the filament to break apart. The dislocated subunit subsequently binds to profilin and facilitates the movement of the subunit to the positive end of the actin filament. Treadmilling is further regulated by a family of proteins called capping proteins. Capping proteins inhibit the addition of subunits to both the positive and negative end of actin. The first protein in this family is called Cap Z which binds the positive end of actin and prevents the addition of subunits. Thus, Cap Z regulates the amount of elongation that occurs in the F-actin fiber. WASp and Rac1 are NPFs that can activate the Arp2/3 complex. NPFs work by binding the actin subunit through the WCA domain, which then activates the Arp2/3 complex by a conformational change in the Arp2 and Arp3 proteins. The Arp2/3 complex then binds to the side of an actin filament by the WH2 domain and establishes a

nucleation point at the positive end of the filament. The nucleation angle of the branching filament and the main actin filament is 70 degrees. Rac1 becomes activated when the CD4 receptor is bound (9). Once bound by Gp120 a messenger protein $G\alpha$ is sent which activates Rho-GTPase which then activates Rac1. Rac1 will activate the Arp2/3 complex and cause branch fibers from the actin filament (9). WASp can nucleate actin fibers and cause branch fibers as well (9). This protein is activated by a Ras related GTP-binding protein Cdc42, the protein will cause a conformational change in WASp which will expose the WH2 domain facilitate actin binding (9). Cdc42 has been shown to interact with SPTBN1 and could influence the replication process of HIV-1 (9). The activation of cofilin and profilin cause the actin filaments to disassemble and elongate. This occurs at the same time the Arp2/3 complex is activated. Cofilin and profilin cause modeling of actin and facilitate the branch fibers produced by the Arp2/3 complex.

HIV-1 uses F-actin and associated proteins in many aspects of infection. The first way it can use the actin cytoskeleton is during fusion of the receptors and co-receptors (70). As stated earlier, the binding of the CD4 receptor sends a signal cascade that activates the Arp2/3 complex. The second process of HIV-1 infection that can utilize F-actin is entry and subsequent fusion of the membranes (70). During entry, the bound CD4 receptor sends a signal cascade that causes reorientation of the actin cytoskeleton. The reorientation of F-actin helps HIV-1 infection by reorganization of the receptor (70). The reorientation of receptors helps with fusion of the membrane by clustering receptors and limiting their lateral movement (70). Once the receptor is bound, Filament A is recruited to the site of entry and binds to the tail of the receptor. The stabilization of the receptor helps with the conformational change in gp41 and fusion of the two membranes (70). The rearrangement of actin to stabilize the receptors and assist with fusion

makes for a convenient way for HIV-1 to migrate to the nucleus. Elongation and disassembly of actin is used to facilitate intracellular transport of vesicles and other products. Previously, the capsid core of HIV-1 was thought to be propelled to the nucleus by actin nucleation and the Arp 2/3 complex. However, the Arp2/3 complex cannot bind to the capsid core directly and must have an adapter molecule of some type. Since SPTBN1 can bind to actin and the capsid core, and can act as a crosslinking protein for actin, SPTBN1 might be involved in viral trafficking by the actin cytoskeleton.

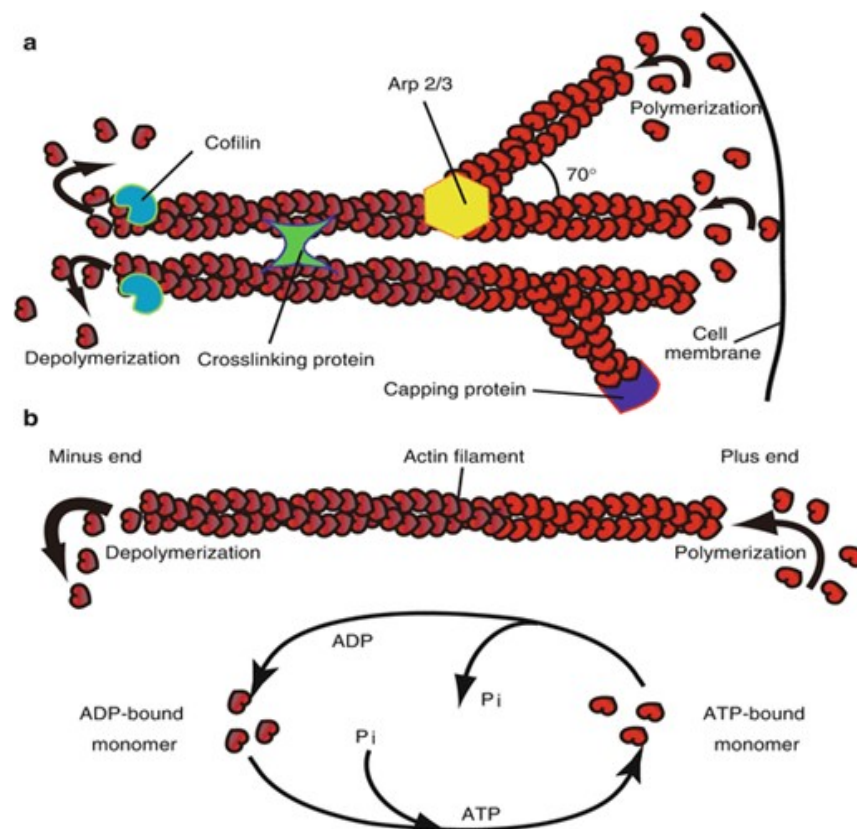


Figure 10. Actin Treadmilling. The diagram shows how treadmilling of the actin cytoskeleton allows the cell to move forward or propel cargo throughout the cell. The negative ended subunits will break off and migrate to the positive end of the actin filament. Once the subunit is attached to the positive end it elongates the strand and propel the cell or cargo forward (B). The figure will also demonstrate how cofilin will degrade the negative end of the filament which also the subunit to migrate to the positive end (A). The figure also demonstrates how the Arp2/3 complex attaches to the main actin filament and polymerizes actin to make branch fibers (96).

Specific Aims and Hypothesis

The role of SPTBN1 in HIV-1 infection remains virtually unknown and unresearched in microglial cells. Understanding the role of SPTBN1 plays in HIV-1 infection will lead to better understanding of host factor interaction in HIV-1 infection, and possibly provide therapy options that decrease the incidence of HAD/HAND.

The first aim of my thesis is to test the effect of SPTBN1 on HIV-1 infectivity of microglial cells. This will be conducted by siRNA knockdown of SPTBN1 in a cultured microglial cell line. Cells will then be infected with VSV-g GFP reporter HIV-1 virus. Flow cytometry will be used to determine the amount of infection by tabulating the number of green cells. The percentage of infected cells will be compared between cells transfected with a SPTBN1 siRNA and cells transfected with a control non targeting siRNA. Downregulation of SPTBN1 will be confirmed by quantitative RT-PCR. I hypothesize that SPTBN1 down regulation in microglial cells will decrease HIV-1 infectivity. Previous studies that also knocked down SPTBN1 saw a decrease in HIV-1 infectivity, regardless of the cell line and HIV-1 virus utilized (8,15,16). I expect the same trend in microglial cells.

The second aim of my thesis is to investigate the effect of SPTBN1 on uncoating kinetics. Since SPTBN1 binds to capsid core protein, there holds the possibility that it participates in some fashion with uncoating of HIV-1. This will be tested by performing a cyclosporin A (CsA) washout assay. The CsA washout assay contains media that has CsA which will inhibit TRIM-CypA. TRIM-CypA binds to the capsid core and prevents the uncoating process. If CsA is in the media, then uncoating will be uninhibited. If the CsA is removed, then all uncoating will stop. Calculations can then be performed to determine the amount of uncoating that has occurred. The calculation will consist of taking the infectivity at a later point (5 hr) and setting it to 100,

meaning that we denoted this time point as 100% of the capsid cores have uncoated. The infectivity at the earlier 30 min and 1 hr time points will be divided by the infectivity at the 5 hr time. This will determine the percent of the capsid cores that have uncoated at that time. First, microglial cells will be transfected with siRNAs targeting SPTBN1 or a control siRNA. After knockdown, microglial cells are infected with VSV-g GFP HIV-1 in the presence of CsA or EtOH only (control). After infection, media that contains CsA is removed at various times, which halts uncoating in the cell. Flow cytometry is used to determine the percentage of infected cells, which is utilized to calculate the percent of uncoating by the calculation above.

I hypothesize that when SPTBN1 is down regulated, uncoating of HIV-1 capsid core will be decreased. According to the Dai publication, SPTBN1 was shown to bind to the capsid protein and nucleocapsid of HIV-1. However, due to SPTBN1 being an adaptor protein, other infection processes of HIV-1 could be affected by SPTBN1 knockdown, without affecting uncoating. For example, SPTBN1 can play a part in other early replication process by acting as an adapter protein which links actin to the capsid core. In the same publication when SPTBN1 was downregulated, an alteration in the actin cytoskeleton occurred. There are other publications that demonstrate that HIV-1 can use actin to facilitate entry, fusion, uncoating and trafficking to the nucleus.

The third aim of my thesis is to determine if viral fusion of HIV-1 is affected by the down regulation of SPTBN1. SPTBN1 was shown to interact with the structures of the actin cytoskeleton which could possibly affect the entry process of the VSV-g HIV, due to actin's interaction with the host membrane (15,16). Fusion must also be tested to confirm the result of the CsA washout assay. Fusion will be tested by the BlaM fusion assay. This assay consists of a dye that will change from green to blue when cleaved by the beta lactamase enzyme. The dye is

inserted inside the cell, and the cell infected with a HIV-1 virus that has a beta lactamase attached to Vpr. Once the HIV-1 virus fuses, Vpr is released and causes the change in color. This assay will start by transfecting microglia cells with siRNAs targeting SPTBN1 or a control siRNA. Two days after transfection the cells will be counted, pelleted, and resuspend in CCF2-AM (fluorescent dye) loading solution for 1 hr, after which the cells pelleted washed and incubated in development media for 16 hr (107). The prepared cells will then be infected with HIV-1 that contains the beta lactamase. Flow cytometry will be used to determine the amount of fusion that has occurred. My hypothesis is that when SPTBN1 is down regulated then fusion of HIV-1 will be decreased which will be marked by a fluorescent different from the control group. The recruitment of actin fibers to the receptor/coreceptor will stabilize and prevent lateral movement. The stabilization of the receptor will help with the conformational change in gp41 which facilitates fusion of the two membranes. In the absent of SPTBN1 the actin cytoskeleton may not stabilize the receptors appropriately and cause altered fusion kinetics of HIV-1.

MATERIAL AND METHODS

Culture and Maintenance of 293T and TCN14 Cells

Culturing HEK 293T cells was accomplished by growing cells in a 10 cm culture dish (Corning) that contained 10 ml of media. The plate was then placed in an incubator set at 37°C and 5% CO₂. Media utilized to grow HEK 293T cells was DMEM (Corning) with 50 ml of fetal bovine serum (FBS; Atlas biological) and 5 ml of penicillin streptomycin glutamine (PSG; Corning) at 1 X concentration. This media will now be referred to as DMEM⁺⁺. The HEK 293T cells were split every three to four days depending on the growth of the cells. When the cells were split it depended on the confluence of the plate which indicates the percent of the plate that was covered by cells. When the plate was 80 to 100% confluent, the plate was split to another 10 cm culture plate.

When HEK 293T cells were split, DMEM⁺⁺ media was aspirated from the dish and 1 ml of trypsin (Corning) was added to the plate. The trypsin was removed with another milliliter of trypsin added and subsequently removed. After the second removal of trypsin, HEK 293T cells were placed in an incubator set at 37°C and 5% CO₂ for two or three mins to allow the cells to dislodge from the plate. While the plate was incubating, 10 ml of DMEM⁺⁺ was added to a new 10 cm culture plate. Once the cells dislodged from the old plate, 10 ml of DMEM⁺⁺ was added back to the dish. Cells were broken up by pipetting the media up and down 3 to 4 times. From the old plate, 1 ml of cells were transferred to the new plate and placed in an incubator at the same standards.

TCN14 cells are derived from the CHME3 microglial cell line to express the restriction factor TRIM-Cyp (106). The human microglial cell line CHME3 was obtained from the Naghavi

Lab at Northwestern University and does not require IRB approval for use (107). TRIM-Cyp is a protein that binds to the intact capsid core of HIV-1. By inserting TRIM-Cyp into microglial cells the uncoating process of HIV-1 can be studied by utilizing the CsA washout assay. TCN14 cells were grown in a 10 cm culture dish and in an incubator with the setting at 37°C and 5% CO₂. The media utilized to grow TCN14 cells was DMEM media with 25 ml of FBS (Atlas biological), 5 ml of PSG at 1 X concentration, and 5 ml of sodium pyruvate (NaPyr; Corning). This media will now be referred to as CHME3 media. Every 3 to 4 days TCN14 cells were split to continue the cell line. When TCN14 cells were split it was based on the confluence of the plate which is the percent of the plate that is covered by cells. When cells were 80 to 100% confluent TCN14 cells were transferred to a new 10 cm culture dish.

To split TCN14 cells CHME3 media was removed, and 5 ml of 1 X PBS (Corning) was added to the plate to neutralize remaining media. The 5 ml of 1 X PBS was removed and 3 ml of trypsin was added to the plate. The plate was then placed in an incubator set at 37°C and 5% CO₂ for 2 or 3 min until the cells dislodged from the plate. While the plate was incubating, 10 ml of CHME3 media was added to a new plate. After the TCN14 cells dislodged from the plate, 7 ml of CHME3 media was added back to the old culture dish. The media was pipetted up and down 4 to 5 times to dislodge the remaining cells adhered to the plate. After TCN14 cells were dislodged, 1 ml of cells were transferred to a new plate and placed in the incubator set at 37°C and 5% CO₂.

Making VSV-g-HIV-GFP Virus

VSV-g pseudotyped HIV-GFP virus is an isolated virus that will be infectious for a single round of infection. The virus will enter the cell via endocytosis and once the virus has

intergraded into the genome it will not produce mature HIV-1 virion. This is due to a mutation in the Env gene which does not allow the virus to produce the envelope of the virus and leads to the single round infectivity. The VSV-g pseudotyped HIV-GFP was made in HEK 293T cells over four-days. On day one, a 100% confluent plate of HEK 293T cells were split in a 1:5 ratio (two ml of DMEM⁺⁺ media/cells were transferred to one of the new plates) and will be called the experimental plate. To another plate, 1 ml of cells were transferred to keep the cell line going and both plates were then placed in an incubator.

On day two, cells in the experimental plate were transfected with two plasmids. The first plasmid contained the genome of HIV-1 with a mutation in the Env gene. The second plasmid contained the VSV-g envelope. The VSV-g envelope came from the vesicular stomatitis virus and allows the HIV-1 virion to enter the cell via endocytosis. It is this plasmid that allows HIV-1 to be infectious for a single round. The transfection mix used to transfect HEK 293T cells consisted of 1 ml DMEM media with no FBS or PSG, 6 µg of HIV-GFP plasmid, 4 µg of CMV-VSV-g plasmid and 40 µl of PEI (Corning). After the transfection mix was made, it was incubated at room temperature for 15 min. The transfection mix added to the experimental plate in a drop wise manner. The cells were left to incubate for 24 hr.

On day three, the media was removed and 10 ml of DMEM⁺⁺ was added to the experimental plate. The plate was placed back into the incubator. On the fourth day, HIV-1 was harvested. Media was taken off by a 10 ml pipette and placed in a 15 ml conical tube (Fisherbrand). Media was then placed in a 20 ml syringe that is attached to a 0.45 µm filter apparatus. The filter apparatus was then attached to a 50 ml conical vial. Media that contained virus was filtered into the 50 ml conical vial. The filtered virus was aliquoted into 9 cryovials. The cryovials were

placed and stored in a cryo-freezer set at -80°C. Safety requirements were followed in compliance with the biosafety protocols approved by Missouri State University.

Testing Infectivity of VSV-g Pseudotyped HIV-GFP Virus

Testing of HIV-GFP was a four-day process which began with a 100% confluent plate that was split by adding 1 ml of cells to the new culture dish to continue the cell line and placed in an incubator. The rest of the cells were placed in a 15 ml conical vial, counted with a hemocytometer, and pipetted into a 96-well plate at 6,000 cells per well. The plate was then placed in an incubator overnight. On the second day the 96-well plate (Falcon) was infected with VSV-g-HIV-GFP. The viruses being tested was the VSV-g HIV and a stock virus utilized as a positive control. To infect HEK 293T cells two solutions were made. The first solution made was 1 X media which was made by 4 ml of DMEM⁺⁺ media and 2 µl of polybrene. The second solution 2 X media was made with 1 ml of DMEM⁺⁺ media and 1 µl of polybrene. The polybrene in each of the solutions aids in infection of VSV-g-HIV. The 96-well plate was removed from the incubator and the DMEM⁺⁺ media was removed. One hundred microliters of 1 X media was added to all the wells that contained cells except for the first well in each row. One hundred microliters of 2 X media was added to the first well in each row. In the first well of each row, 100 µl of VSV-g-HIV-GFP virus was added. To the first well in the second row, 100 µl of positive control virus was added. To the last row, HIV-1 was not added and utilized as a negative control. A serial dilution was made by taking 100 µl of sample from the first well and transferring it to the following well. This trend was carried out across the plate. The last 100 µl from the well was discarded in 10% bleach. The plate was then place in an incubator overnight.

On the third day, media from the wells was removed and 200 μ l of DMEM⁺⁺ was added to each of the wells. The plate was placed back into the incubator. On the fourth day cells were harvested and fixed in solution. The plate was removed from the incubator and media was removed. To each well 100 μ l of trypsin was added and the plate was placed in an incubator for 2 to 3 min. After incubation, the plate was removed, and the cells were resuspended. After the cells were resuspended, 100 μ l of cell fix was added to the wells. Cell fix was made by one-part paraformaldehyde (Chem Cruz) and one-part 1 X PBS. The plate was wrapped in parafilm and foil and placed at 4°C. After an overnight incubation, the number of infected cells in the fixed samples was determined by flow cytometry. Infected cells were identified based on the GFP signal that was expressed by infected cells. The cells expressed GFP when they are infected with HIV due to the GFP gene being integrated in the genome of HIV. Once the genomic material of HIV integrates in the host the cell will express GFP. The percent infectivity was calculated as a percent by the Csampl software on the flow cytometer (BD Accuri C6sampl).

SiRNA Knockdown of SPTBN1

SPTBN1 knockdown in TNC14 cells consisted of a two-day protocol. On the first day, a confluent plate of TCN14 cells was split and 1 ml of cells was transferred to a newly prepared plate to continue the cell line. The remaining cells were counted via a hemocytometer and plated to 1.7×10^5 cell per well in a 6-well dish (Falcon). On the second day, cells in the 6-well dish were transfected with a pool of siRNA for SPTBN1. To transfect TCN14 cells, the tissue culture hood along with all equipment was wiped down with RNase Away (Invitrogen) and UV-treated for 15 min. While the hood was being sanitized, the pool of siRNA along with all reagents was removed from the -20°C freezer and thawed on ice. The siRNA was centrifuged, and cells were

checked to make sure the 6-well plate was 60 to 80% confluent. For each siRNA condition, two Eppendorf tubes (Fisherbrand) were used, tube 1 and tube 2. To tube 1, 50 μ l of OPTIMEM (Gibco) and 4 μ l of lipofectamine were added. To tube 2, 100 μ l of OPTIMEM and 3 μ l of siRNA were added. Both tubes were left to incubate for 5 min at room temperature. The siRNA conditions used for this experiment was Spectrin beta non-erythrocytic 1 (SPTBN1), Trim-Cyp for a positive control, non-Target 4 (NT4) for a negative control and no siRNA as a negative control. The orientation of the plate can be found in (Figure 11). After the 5 min incubation period, tube 1 was added to tube 2 and then incubated for 20 min. During the 20 min incubation, CHME3 media was removed and 1 ml of OPTIMEM was added to each of the wells. After the 20 min incubation period the contents of the Eppendorf tube was added to the well in a drop wise manner. The 6-well plate was placed back in the incubator. After 4 hr the plate was removed and 1 ml of CHME3 media without PSG was added to each well and placed back in the incubator. The SPTBN1 knockdown TCN14 cells were then utilized in the infectivity and a mini-uncoating assay.

| | | |
|----------------------|-----------------|-------|
| SPTBN1 | NT4 (- control) | Cells |
| Trim-Cyp (+ control) | No siRNA | Empty |

Figure 11. Schematic of Knockdown Plate. The figure shows the orientation of a 6-well of where the knockdown cells are located, and which are controls for the experiment. Trim-Cyp is used as a negative control and NT4 was utilized as a positive control.

HIV-1 Infectivity of SPTBN1 Knockdown Cells

To test HIV infectivity, the day after the knock down procedure was performed, cells were transferred to a 96-well plate (Falcon). To transfer TCN14 cells, media in the 6-well plate was removed and 2 ml of 1 X PBS was added to each well to neutralize any remaining media. The 1 X PBS was aspirated, and 1 ml of trypsin was added to each of the wells. The plate was

place in an incubator for 2-3 min to allow the cells to dislodge from the plate. After incubation, 1 ml of CHME3 media was added to the wells and each siRNA condition was separated into 15 ml conical vials. Each siRNA condition was counted by a hemocytometer and plated at 6,000 cells per well. The cell/media solution was transferred to a 96-well plate at 100 μ l per well and placed in an incubator.

The next day, cells were infected with VSV-g pseudotyped HIV-GFP. To infect TCN14 cells, a spinoculation mix was made up of polybrene, CsA 2.5 μ m (Sigma-Aldrich) or EtOH, HIV-GFP and CHME3 media. Four master mixes of the spinoculation mix were made: tube 1 contained CsA with HIV-GFP, the second tube contained EtOH with HIV-GFP, the third tube contained CsA with no HIV and the fourth tube contained EtOH with no HIV. The two non-HIV containing tubes were utilized as negative controls. The media utilized for each condition were left cold to prevent fusion of HIV during spinoculation. The plate was removed from the incubator and CHME3 media was removed. One hundred microliters from each tube was added to three wells each. The setup of the plate can be seen in (Figure 12). The plate was placed in a centrifuge cooled at 16°C and spun at 1200 g for 1 hr. After inoculation, the spinoculation mix was aspirated and replaced with warm CHME3 media of the same type but did not contain HIV-GFP. The plate was placed in the incubator overnight. The following day media was removed and replaced with 200 μ l of CHME3 media. On the final day, cells were harvested and fixed with cell fix solution. First, media was removed and 100 μ l of trypsin was added to the wells. The plate was placed back in the incubator for 2-3 min to allow the cells to dislodge from the plate. After the cells were dislodged 100 μ l of cell fix was added to the wells. Cell fix solution contained one-part paraformaldehyde and one-part 1 X PBS. The plate was sealed with parafilm and wrapped in foil and placed in the fridge overnight. After an overnight incubation, the number

of infected cells in the fixed samples was determined by flow cytometry. Infected cells were identified based on the GFP signal, which has an excitation wavelength of 510 nm and expressed by infected cells. The cells expressed GFP when they are infected with HIV due to the GFP gene being integrated in the genome of HIV. Once the genomic material of HIV integrates in the host the cell will express GFP. The percent infectivity was calculated as a percent by the C-sampler software on the flow cytometer (BD Accuri C6sampler). When the siRNA knockdown cells were analyzed, the infectivity can be determined, and samples were normalized to NT4.

| | | | | | | | |
|-------|----------|---------|---------|----------|----------|----------|-------|
| Empty | CsA- HIV | CsA-HIV | CsA-HIV | EtOH-HIV | EtOH-HIV | EtOH HIV | Empty |
| Empty | CsA | CsA | CsA | EtOH | EtOH | EtOH | Empty |

Figure 12. Plate Set up of Testing Infectivity. Below shows the orientation of the 96-well plate. Each of the conditions were done in triplicate and consisted of CsA with HIV, EtOH with HIV, CsA without HIV and EtOH without HIV. Both conditions that contained no HIV were utilized as negative and EtOH were used as a positive control.

Mini-CsA Washout Assay and Construction of Primers

To perform a mini-CsA washout assay, knockdown cells were first transferred from a 6-well plate to a 96-well plate. The transferring of cells was conducted by the same protocol as testing infectivity of SPTBN1 knockdown cells. With the mini-uncoating, eighty wells were needed to complete the assay for all timepoints and controls. The conditions tested in cells were conducted in the presence of CsA and EtOH. The various knockdown of TCN14 cells consisted of SPTBN1, CypA, NT4, and no siRNA. The orientation of conditions and siRNA knockdown can be seen in (Figure 13). CsA was utilized to inactivate Trim-Cyp, in the presents of CsA Trim-Cyp will not bind to the capsid core and uncoating will occur. When CsA is removed Trim-Cyp can bind to the capsid core and halt the uncoating process. The removal of CsA at various time points allowed uncoating to be tabulated at various times. EtOH is used to dissolve CsA and

was used as a control. The NT4 knockdown cells were transfected with a siRNA that does not target any RNA in the cell and was used as a positive control. After the cells were separated by siRNA conditions and plated at 6,000 cells per well, the plate was placed in the incubator overnight. The following day the cells were infected with HIV by the same protocol as testing infectivity of SPTBN1 knockdown cells. Once the wells were infected, the plate was placed in the incubator. At time points 30 min, 1 hr and 5 hr time points, CsA media was removed and replaced with 200 μ l of CHME3 media. The mini-uncoating assay can be conducted at the same time as testing infectivity to save on resources. Media on the negative controls were replaced at the same time as the 5 hr time point. If conducting the infectivity assay at the same time, the wells utilized for infectivity were changed with media at the same time as the negative control and 5 hr time point. After the media was replaced, the plate was placed back in the incubator. On the following day, CHME3 media was aspirated and replaced with fresh CHME3 media. The plate was then placed back into the incubator overnight. The next day TCN14 cells were harvested by the same protocol in testing infectivity of SPTBN1 knockdown cells. The following day flow cytometry was performed and followed the same protocol as stated in testing infectivity of SPTBN1 knockdown cells.

| | CsA | | EtOH | | | |
|----------|--------|--------|--------|--------|--------|--------|
| 30 min | SPTBN1 | SPTBN1 | SPTBN1 | SPTBN1 | SPTBN1 | SPTBN1 |
| 1 hr | SPTBN1 | SPTBN1 | SPTBN1 | SPTBN1 | SPTBN1 | SPTBN1 |
| 5 hr | SPTBN1 | SPTBN1 | SPTBN1 | SPTBN1 | SPTBN1 | SPTBN1 |
| 30 min | NT4 | NT4 | NT4 | NT4 | NT4 | NT4 |
| 1 hr | NT4 | NT4 | NT4 | NT4 | NT4 | NT4 |
| 5 hr | NT4 | NT4 | NT4 | NT4 | NT4 | NT4 |
| Neg con. | SPTBN1 | SPTBN1 | SPTBN1 | SPTBN1 | SPTBN1 | SPTBN1 |
| Neg con. | NT4 | NT4 | NT4 | NT4 | NT4 | NT4 |

Figure 13. Mini-Uncoating CsA Washout Plate. Below shows the orientation of the CsA washout plate. CsA was used to bind to Trim-Cyp and facilitate uncoating. When CsA is removed Trim-Cyp can bind to the capsid core and halt uncoating. The knockdown cells were also conducted in the presents of EtOH and was used as a negative control. At the 30 min, 1 hr, 5 hr time points the media was removed and 200 µl of CHEM3 was added. At the 5 hr time mark the negative control had the media removed and replaced. The same setup was conducted for CypA and no siRNA.

To make primers for SPTBN1, the amino acid (AA) sequence of the protein, mRNA, and genomic sequence of SPTBN1 was found in the NCBI database (NM_003128.3). The first hit for each was chosen and recorded along with the e-number, app number, percent identity. The sequence of each was placed in a word document for future analysis. Once the sequences were found the domains of each was found utilizing PROSITE. The genomic sequence was placed into MEGA X to find the introns and exons. The section was analyzed to find areas that were close together and not in the domains of the genomic DNA or the mRNA sequence of SPTBN1. The sequences were placed into primer 3D and primers were made and recorded. The annealing was set 54-62°C, CG content was set between 20-80% and the length was set between 24-30 BP. The reverse was made by reversing and complementary BP of the sequence in the cDNA and gDNA sequence. The sequence of both primer sets can be found in (Figure 14).

| Primers | Sequence |
|-----------------------|-------------------------------------|
| Forward primer SPTBN1 | 5'-GCA CAC TAC ATT TGA GCA TGA C-3' |
| Reverse Primer SPTBN1 | 5'-GTT CTC GCG CTT CTG GAT A-3' |
| Forward Primer GAPDH | 5'-GCA CCG TCA AGG CTG AGA AC-3' |
| Reverse Primer GAPDH | 5'-GCC TTC TCC ATG GTG AA-3' |

Figure 14. Primer Sequences. In the diagram it shows the sequence of the forward and reverse primers for SPTBN1 and GAPDH.

Confirmation of Primer and Determining Annealing Temperature SPTBN1 and GAPDH

To confirm the annealing temperature of primers utilized for SPTBN1 and GAPDH, the hood was first wiped down with RNase and UV-treated for 15 min. All equipment utilized for the experiment followed the same standard. The materials were thawed on ice and included the forward/reverse primers for SPTBN1 or GAPDH, Go-Taq DNA Polymerase (Promega), ddH₂O, and pGEMTeasy-SPTBN1 plasmid (6.2960 µg/µl) or the pGEMTeasy-GAPDH plasmid (0.8994 µg/µl). The sequence of the primer (Integrated DNA Tech) sets can be found in Figure 14. Once the hood was sanitized a master mix was made, for one reaction 12.5 µl of 2.5 X Go-Taq DNA polymerase, 0.5 µl of 20 µM forward/reverse primers for SPTBN1 or GAPDH, 5 µl of pGEMteasy SPTBN1 or pGEMteasy GAPDH plasmid and 6.5 µl of ddH₂O. Twenty-five microliters were placed in PCR tubes and placed in a thermocycler (Bio-Rad). Each of the reaction conditions were done in triplicate. The denaturing step was set at 95°C for 0.5 min, the annealing temperature was set as a gradient from 57-67°C for 0.5 min, the elongation temperature was set at 65°C for 0.5 min. After PCR was complete, the product which was 20 µl was ran on a 3% agarose gel made with 1 X TAE and EtBR. The buffer used to run the gel was 1 X TAE and was ran on 110 V for 45 min. The gel was imaged utilizing Gel logic 2000 imager.

Primer Efficiency and Confirming siRNA Knockdown

To determine primer efficiency, plasmid pGEMteasy SPTBN1 or pGEMteasy GAPDH was placed in the nanodrop to determine the quantity and quality of the plasmids. The quantity of SPTBN1 plasmid was 6.2960 µg/µl and GAPDH plasmid was 8.99 µg/µl. For each plasmid, dilution was made from 10^{-1} - 10^{-8} which correspond to concentration from 0.62960-6.2960 x 10^{-8} µg/µl for SPTBN1 and 0.899-8.99 x 10^{-8} µg/µl for GAPDH. For qPCR, all materials were collected and stored on ice which included Ssofast (Bio-Rad), nuclease free water (Promega), forward/reverse primer for SPTBN1 or GAPDH, and plasmid DNA dilutions for SPTBN1 or GAPDH. After the materials were thawed a master mix was made, that contained (per reaction) 10 µl of Ssofast, 0.5 µl of forward/reverse primer for SPTBN1 and GAPDH, 5 µl of DNA dilutions for SPTBN1 and GAPDH, and 4 µl of ddH₂O. Each reaction was done in triplicate. There was a well that contained 5 µl of ddH₂O instead of DNA and utilized as a negative control. To each well 15 µl of master mix was added along with 5 µl of DNA dilution. The wells were sealed and centrifuge at 300 g for 1 min. The reactions were placed in the thermocycler (Bio-Rad). Denaturing was set at 95°C for 30 sec, annealing was set at 60°C for 30 sec and the elongation was set at 65°C for 30 sec. The number of cycles ran in the thermocycler was 45 and the data was exported to excel. To determine primer efficiency, a C_q mean was conducted by averaging the C_q dilution triplicate and plotting it on a scatter plot with the DNA dilutions. A trendline was added to the graph along with the slope and the R² value. To get the primer efficiency (E) value, the equation $E = 10^{(-1/\text{slope})} - 1$ was utilized. The E value for GAPDH was 0.74 and 1.05 for SPTBN1.

To confirm SPTBN1 knockdown in TCN14 cells, the procedure started with the transfer of cells from a 10 cm dish to a 6-well plate and consisted of a 5-day process. The first day started with the transferring of cells to a 6-well plate from a 10 cm dish by the previously described

procedure in knockdown of TCN14 cells. The following day, cells were transfected by a siRNA (SPTBN1, NT4, no siRNA) by a previously described procedure in knockdown of TCN14 cells. On the third day media was changed and placed back in the incubator overnight. On the fourth day wells were harvested and infected with HIV-GFP. The cells were infected to determine how the amount of knockdown correlates with HIV infection. Cells were harvested by adding 1 ml of trypsin and allowing cells to dislodge from the plate for 2-3 min. TCN14 cells were then removed from the well and placed in a 15 ml conical vial and counted by a hemocytometer. Some of the cells were plated at 6,000 cells per well and was placed back in the incubator and utilized to test for infectivity. The rest of the cells were utilized to obtain RNA and monitor the amount of SPTBN1 knockdown.

The RNA easy kit from Qiagen was used to obtain RNA. Cells were counted in a hemocytometer and 5.0×10^6 cells were placed in a 15 ml conical vial. The vial was centrifuged to pellet cells and the supernatant was poured off without disturbing the pellet. The pelleted cells were resuspended with 350 μ l of RTL/BME buffer (Qiagen) and the contents were transferred to an Eppendorf tube. To the tube, 70 μ l of EtOH was added to the lysate and mixed. The lab area was prepared for RNA work by wiping down the bench with RNase. Seven hundred microliters of sample were transferred to a RNeasy spin column (Qiagen) and place in a 2 ml collection tube (this includes any precipitate that may have formed). The spin column was centrifuged for 15 sec at 10,000 rpm and the flow through was discarded. Ten microliters of DNase stock were added to 70 μ l of buffered solution RDD, the solution was then mixed by inverting the tube. The newly made solution was centrifuged to bring the liquid to the bottom of the tube. The DNase solution was added directly to the RNeasy spin column membrane and incubated for 15 min at room temperature. Following the incubation period, 350 μ l of RW1 buffer was added to the RNeasy

spin column and centrifuge for 15 sec at 10,000 rpm. The flow through was discarded. In the subsequent step, 500 µl of RPE buffer was added to the spin column and centrifuged for 2 min at 10,000 rpm. The spin column was transferred to a new 2 ml collection tube and the old tube was discarded. The spin column was centrifuged at max for 1 min, after which the flow through was discarded. The spin column was then transferred to a 1.5 ml collection tube and 30-50 µl of RNase-free water was placed directly to the spin column membrane. The spin column was centrifuged for 1 min at 10,000 rpm to elute RNA. The RNA was labeled and stored at -4°C in sample box. The RNA extracted was reverse transcribed into cDNA later.

To make cDNA, the fume hood was wiped down with RNase and UV treated for 15 min. All equipment utilized for the experiment followed the same protocol. After the hood was treated two separate master mixes were made, Rt (+) and Rt (-). The common components for each mix consist of 4 µl of AMV buffer, 2 µl MgCl₂, 2 µl of 20 µM dNTPs, 1 µl of RNasin, 2 µl of oligodT, 4 µl of 20 µM knockdown RNA samples (SPTBN1, NT4, no siRNA) and H₂O utilized to 20 µl. The amounts listed for each component was for one reaction. The component that changed between the two-master mixes was AMV RT, the Rt (+) contained 4 µl of the solution and the Rt (-) master mix contained an extra 4 µl of H₂O. For each siRNA knockdown condition, 16 µl was aliquoted into microcentrifuge tubes and allowed to incubate for 1 hr at 42°C. After the incubation period the made cDNA was stored in -20°C.

To determine the amount of SPTBN1 knockdown, qPCR was ran on the Rt (+) and Rt (-) cDNA. To conduct PCR a master mix was made which consisted of 10 µl of Ssofast, 0.5 µl of 20 µM forward and reverse primers for GAPDH and SPTBN1, 8 µl of H₂O. The amounts listed were for one reaction and each reaction condition was done in triplicate. After the master mix was made, 19 µl of the mix was aliquoted into PCR tubes along with 1 µl cDNA. The orientation

of the tube and samples can be found in (Figure 15). The tubes were sealed the tubes were spun in a centrifuge at 300 g for 1 min and transferred to a thermocycler. PCR was ran on the samples utilizing the protocol found in primer efficiency. After PCR was complete the data was exported to excel, and the triplicate of each run was averaged together. The ΔC_q was determined for each of the samples by taking the NT4 +RT sample and subtracting the SPTBN1 knockdown cells. This was done with GAPDH and SPTBN1 primers. The E value for both SPTBN1 and GAPDH had one added to the number which is part of the formula for the Pfaffl method. The ΔC_q was then taken to the power of the efficacy that was just calculated. The same process was done using SPTBN1 primers. The number calculated using SPTBN1 primer was divided by the number calculated using GAPDH primers to get the amount of knockdown seen in SPTBN1 knockdown cells.

| Tube strip | Tube strip condition | | | | | | | |
|------------|----------------------|------------|------------|------------|------------|------------|------------------|-------|
| 1 | SPT Rt (+) | SPT Rt (-) | NT4 Rt (+) | NT4 Rt (-) | Non Rt (+) | Non Rt (-) | H ₂ O | Empty |
| 2 | SPT Rt (+) | SPT Rt (-) | NT4 Rt (+) | NT4 Rt (-) | Non Rt (+) | Non Rt (-) | H ₂ O | Empty |
| 3 | SPT Rt (+) | SPT Rt (-) | NT4 Rt (+) | NT4 Rt (-) | Non Rt (+) | Non Rt (-) | H ₂ O | Empty |

Figure 15. Orientation of KD Confirmation. Orientation of the tube strips that was utilized for confirming knockdown of SPTBN1 and performed in triplicate. In the first two wells contains knockdown cells for SPTBN1, the following two wells contained knockdown cells for the non-target 4 sequence. The following two wells were transfected with no siRNA, the last tube contained H₂O which was utilized as a control. The Rt (+) samples were the samples that were reverse transcribed into DNA. The Rt (-) sample had no reverse transcriptase in the reaction and were not made into DNA and was utilized as a control.

RESULTS

SPTBN1 Knockdown Effect on Infectivity

siRNAs were utilized to knockdown SPTBN1 so that its role in various process of HIV-1 replication can be explored. The infectivity of HIV was tested in TCN14 cells which are CHME3 cells that have Trim-Cyp inserted. To test the infectivity of HIV-1, SPTBN1 was knocked down by a pool of four siRNAs. A control no siRNA treatment utilized water instead of a siRNA to make sure that the siRNA transfection process does not affect the cell. A non-targeting siRNA (NT4) was used as a negative control to make sure that a siRNA does not affect the cell and interfere HIV-1 replication. Once the cells were transfected with the siRNAs, TCN14 cells were infected with HIV-GFP and flow cytometry used to determine the amount of GFP, and therefore infectivity in each condition. For one run SPTBN1 knockdown, the infectivity was 27.57%, while NT4 control and no siRNA controls were 35.05% and 42.77%, respectively (Table 1A). To determine the percent of cells that were infected with HIV and to compare samples, the data was normalize to NT4 control. For one run, SPTBN1 cells infectivity was 78.6%, when compared to the NT4 control, the no siRNA sample was at 108% when compared to the NT4 control (Table 1A). The experiment was conducted two times and averaged together to get averaged infectivity for each condition (Table 1B and Figure 16). These results show that when SPTBN1 is down regulated there is a decrease in the amount of HIV infectivity. When the normalized data from the SPTBN1 condition was compared to the NT4 control there was a decrease of 19.75% in the amount of infectivity of HIV- GFP (Table 1B and Figure 16).

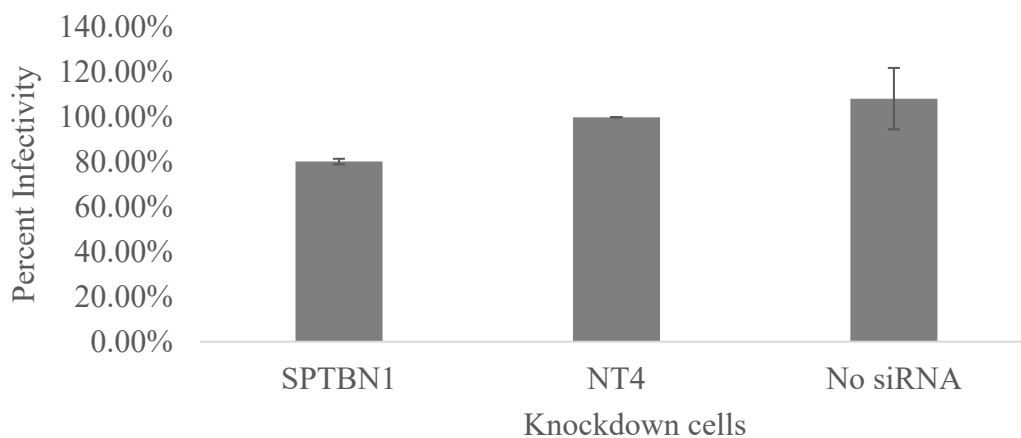


Figure 16. Graph of Normalized Infectivity with SiRNA Knockdown. Average infectivity seen by the knockdown cells. The data were normalized to the NT4. Error bars shows the standard error in each sample. N = 2.

Table 1. Effects of HIV Infectivity in SPTBN1 Knockdown Cells. Part A shows the unnormalized raw infectivity data which indicates the percent of cells that were infected with HIV. The second part of the table show the normalized data from infected cells by dividing the infectivity of the SPTBN1 cell by the infectivity of the NT4 control. Part B shows the average of the normalized data of the 2 separate runs in SPTBN1 knockdown cells when compared to the NT4 control.

A)

| Sept 23, 2019, infectivity assay | | | |
|---|--------|---------------|----------|
| Sample | SPTBN1 | NT4 (control) | No siRNA |
| Percent infectivity | 27.57 | 35.07 | 42.77 |
| Sept 23, 2019, infectivity assay- data normalized | | | |
| SPTBN1 | NT4 | No siRNA | |
| 79% | 100% | 122% | |

B)

| Averaged normalized infectivity assay (duplicated experiment) | | | |
|---|--------------|--------------|---------|
| | Sept 23 2019 | Oct. 18 2019 | Average |
| SPTBN1 | 79% | 81.5% | 80.25% |
| NT4 | 100% | 100% | 100% |
| No siRNA | 122% | 94.6% | 108.3% |

Confirming the Annealing Temperature of Primers

Once the infectivity was determined, we next sought to confirm knockdown of SPTBN1 in TCN14 cells by utilizing quantitative PCR. The reason for calculating the annealing temperature and primer efficacy is to use the Pfaffl method which will allow a comparison to be made between a housekeeping gene (GAPDH) and SPTBN1 knockdown. This method will also control for the varying number of cells between SPTBN1, NT4, and no siRNA samples. To confirm the annealing temperature, qPCR was conducted on pGEM plasmids that contained either SPTBN1 or GAPDH sequence. When qPCR was conducted the annealing temperature was set as a gradient from 57-67°C (Figure 17). The qPCR products were separated by electrophoresis on an agarose gel, and the predicted value was determined to be 125 bp. The band where there was a decrease in the intensity was where the annealing temperature was no longer optimal (Figure 17). This was due to primers not binding optimally due to the increased temperature. The band before this decrease was the optimal annealing temperature for SPTBN1 and GAPDH because it was able to produce the most product. The optimal annealing temperature for both SPTBN1 and GAPDH was determined to be 60°C (Figure 17).

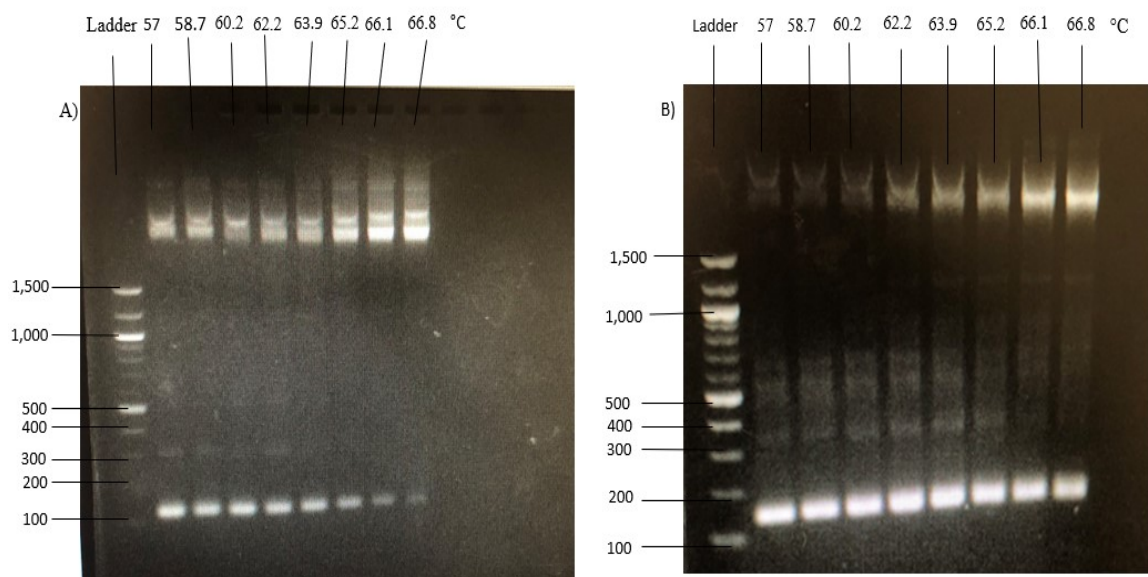


Figure 17. Annealing Temperature Confirmation for SPTBN1 and GAPDH primers. Gels used to determine the annealing temperature for SPTBN1 (A) and GAPDH (B) primers. PCR was run with each primer set with the predicated value of 125 and a gradient of different annealing temperatures (temperature shown at the top of the gel). PCR products were run out on the gel. The base pairs used for the ladder are found in the left-hand side of the gel.

Determining Primer Efficacy for SPTBN1 and GAPDH

After the annealing temperature was confirmed at 60°C, the primer efficiency was calculated. To obtain the primer efficiency, a pGEM plasmid containing either SPTBN1 or GAPDH sequence was diluted from 10^{-1} to 10^{-8} . The dilutions were ran through quantitative PCR in triplicate (Table 2A, Table 3A, Figure 18, Figure 20A). The C_q value for each reaction of the triplicate was then averaged (Table 2B and Table 3B). These data points were plotted on a scatter plot and a line of best fit was drawn (Figure 19A and Figure 20B). The primer efficiency was calculated by inputting the slope of the line of best fit into the equation $10^{(-1/\text{slope})}$ - (Figure 19B and Figure 20C). For SPTBN1, the primer efficiency was 1.05 (Figure 19B). GAPDH primers had an efficiency of 0.77 (Figure 20C).

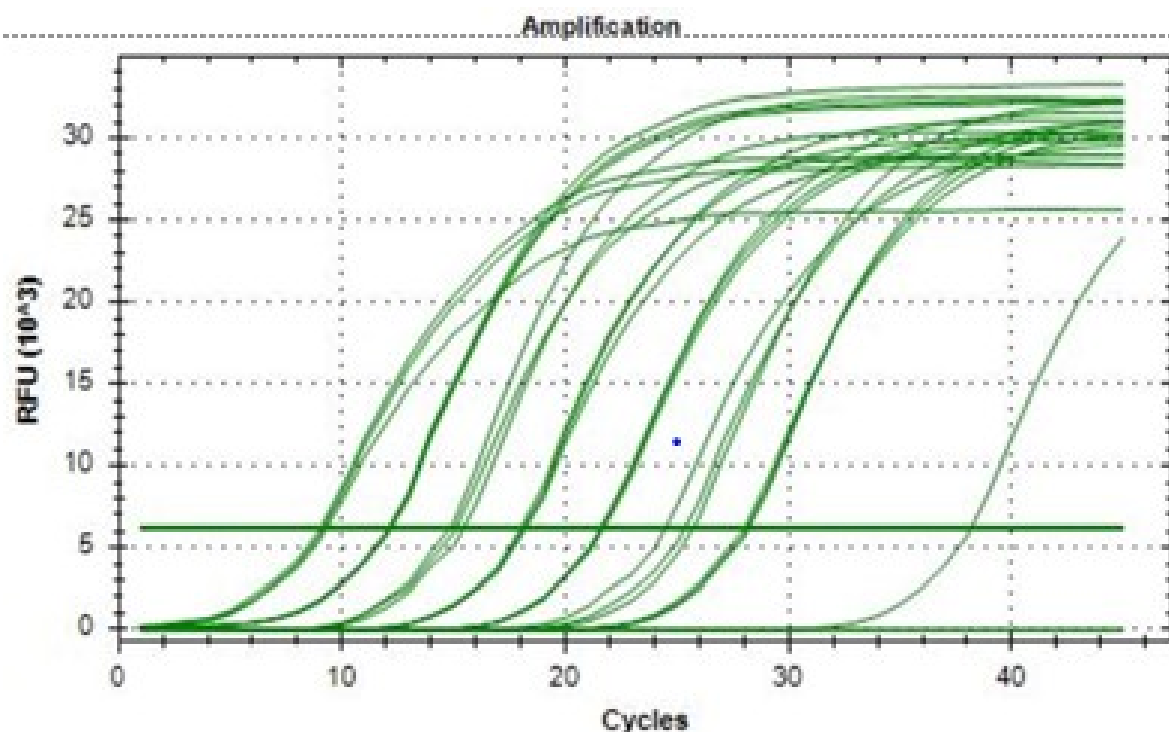


Figure 18. Amplification Curve for SPTBN1 Primers to Determine Primer Efficiency. Amplification curve of qPCR of each DNA dilutions for SPTBN1. Each dilution was done in triplicate and span from $0.8994\text{--}8.994 \times 10^{-8} \mu\text{g}/\mu\text{l}$.

Table 2. Primer Efficiency of SPTBN1 Primers. Part A shows the raw data obtained from one run. Each dilution was done in triplicate and water was utilized as a negative control. Part B shows the averaged data for each DNA dilution. The data will then be utilized to obtain a primer efficacy for SPTBN1.

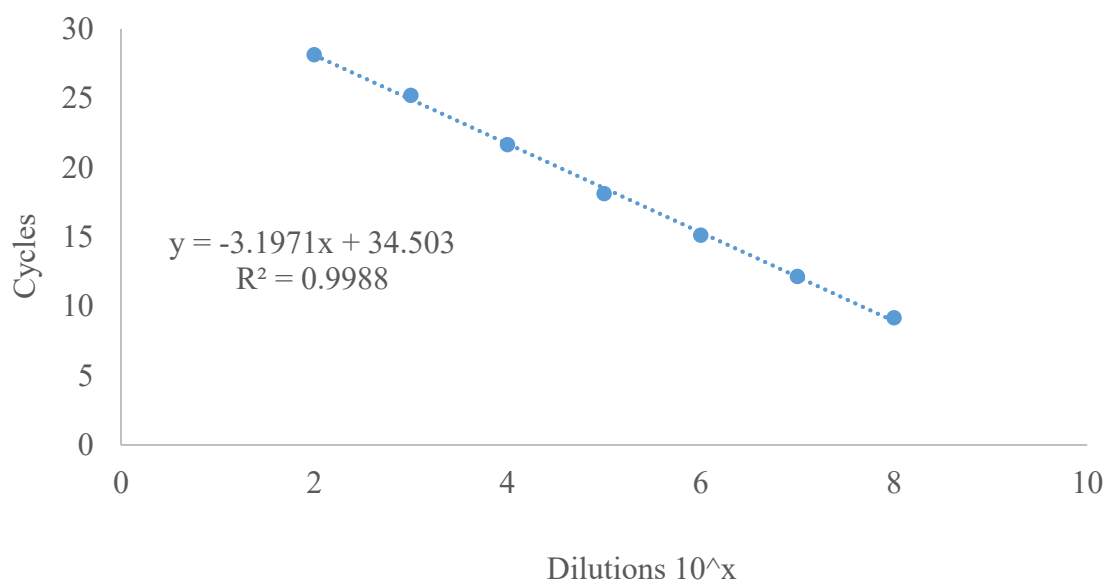
A)

| Cq for SPTBN1 | | |
|----------------------|--------------|-----------|
| Well | Fluor | Cq |
| A01 | SYBR | 9.31 |
| A02 | SYBR | 9.18 |
| A03 | SYBR | 9.05 |
| A04 | SYBR | 12.12 |
| A05 | SYBR | 12.16 |
| A06 | SYBR | 12.24 |
| A07 | SYBR | 14.85 |
| A08 | SYBR | 15.12 |
| B01 | SYBR | 15.46 |
| B02 | SYBR | 18.15 |
| B03 | SYBR | 18.24 |
| B04 | SYBR | 18.02 |
| B05 | SYBR | 21.59 |
| B06 | SYBR | 21.75 |
| B07 | SYBR | 21.63 |
| B08 | SYBR | 24.51 |
| C01 | SYBR | 25.75 |
| C02 | SYBR | 25.38 |
| C03 | SYBR | 28.05 |
| C04 | SYBR | 28.19 |
| C05 | SYBR | 28.22 |
| C06 | SYBR | 38.19 |

B)

| Averaged Cq for SPTBN1 | |
|-----------------------------------|----------------|
| Dilution (10^{-X}) | Cq mean |
| 8 | 9.18 |
| 7 | 12.16 |
| 6 | 15.14 |
| 5 | 18.13 |
| 4 | 21.65 |
| 3 | 25.21 |
| 2 | 28.15 |

A)



B)

Primer efficiency calculation SPTBN1 (Pfaffl method)

| Slope | R ² | Efficacy Calculation |
|-------------------------|----------------|-----------------------------|
| $Y = -3.1971x + 34.503$ | 0.9988 | $10^{(-1/-3.197)-1} = 1.05$ |

Figure 19. Primer Efficacy Calculation and Graph for SPTBN1 Primers. (A) Scatter plot of the averaged Cq value for each DNA dilution for SPTBN1. The graph also shows the equation which yield the line of best fit. The graph also has the R^2 value which indicates how well the plotted points line up with the line of best fit. (B) The primer efficacy was calculated by inputting the slope obtained from the line of best fit into an equation utilized by the Pfaffl method.

Table 3. Primer Efficacy for GAPDH Primers. Part A shows the C_q from qPCR of GAPDH DNA dilutions. Part B shows the averaged C_q mean for each GAPDH dilution sample. The data from the averaged DNA dilution were used to obtain the primer efficacy for GAPDH.

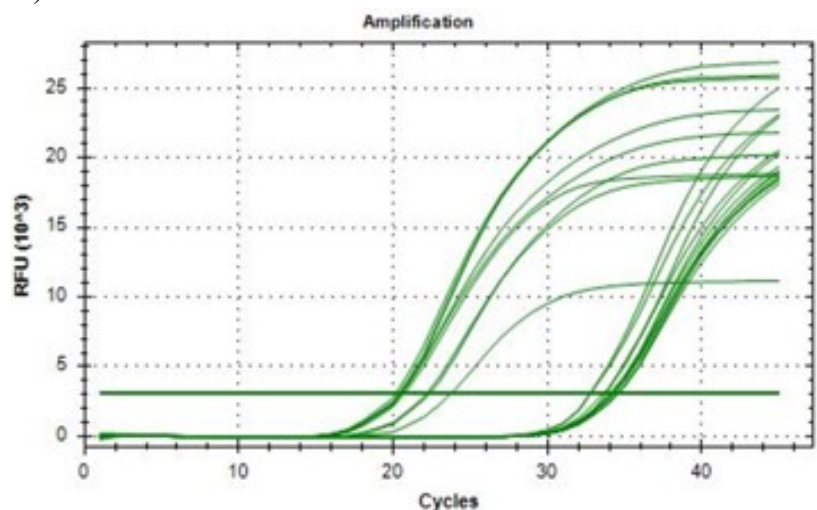
A)

| C_q for GAPDH | |
|--------------------------------|--------------|
| Well | Fluor |
| A01 | SYBR |
| A02 | SYBR |
| A03 | SYBR |
| A04 | SYBR |
| A05 | SYBR |
| A06 | SYBR |
| A07 | SYBR |
| A08 | SYBR |
| B01 | SYBR |
| B02 | SYBR |
| B03 | SYBR |
| B04 | SYBR |
| B05 | SYBR |
| B06 | SYBR |
| B07 | SYBR |
| B08 | SYBR |
| C01 | SYBR |
| C02 | SYBR |
| C03 | SYBR |
| C04 | SYBR |
| C05 | SYBR |
| C06 | SYBR |

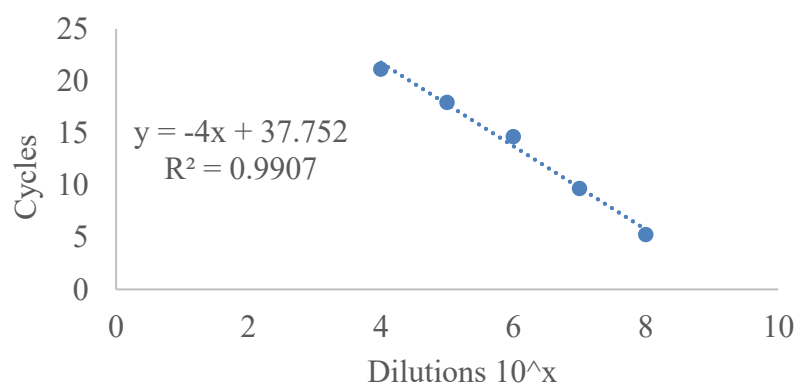
B)

| Average C_q for GAPDH | |
|--|---------------------------|
| Dilution (10^{-x}) | C_q mean |
| 8 | 5.27 |
| 7 | 9.71 |
| 6 | 14.68 |
| 5 | 17.95 |
| 4 | 21.15 |
| 3 | 26.38 |
| 2 | 27.43 |

A)



B)



C)

Primer efficacy calculation GAPDH (Pfaffl method)

| Slope | R ² | Efficacy Calculation |
|-----------------------|----------------|-------------------------|
| Y=-4x + 37.752 | 0.9907 | $10^{(-1/-4)-1} = 0.77$ |

Figure 20. Primer Efficacy Calculation and Graph of GAPDH Primers. (A) The qPCR amplification curve of each GAPDH DNA dilutions. Each dilution was done in triplicate and span from $0.629-6.29 \times 10^{-8} \mu\text{g}/\mu\text{l}$. (B) The graph of the averaged C_q for each DNA dilution for the GAPDH primers. The slope and R² value which were obtained from the line of best fit which was drawn between the plot dilution points for GAPDH. (C) The primer efficacy was calculated by putting the calculated slope into an equation utilized by the Pfaffl method.

Confirming Knockdown of SPTBN1

After the primer efficiency was determined for SPTBN1 and GAPDH primers, the amount of knockdown in TCN14 cells can be determined. RNA was extracted from the cells and reverse transcribed to cDNA. A control for RT-PCR was used in which some RNA was not reverse transcribed into cDNA by neglecting to add reverse transcriptase (RT) to the reaction. This control set is referred to as RT- (Table 4A). qPCR was performed on the cDNA utilizing SPTBN1 or GAPDH primer sets. Each sample was tested in triplicate, and the data averaged (Table 4A, Table 4B, Table 5A and Table 5B). Based on the Pfaffl method, SPTBN1 was knocked down by 38.7% in the siRNA knockdown samples (Table 4B and 6). When the infectivity was tested in the knockdown cells, it correlated to a decrease of 37.58% (Table 6 and Figure 21).

Table 4. Confirming Knockdown of SPTBN1. SPTBN1 was quantified utilizing the Pfaffl method. Part A shows the Cq from qPCR conducted on cDNA made from knockdown and control cell types. Each sample contained a RT+ and RT- sample, which was used as a control. Part B quantifies the level of knock down, calculated by the Pfaffl method. The ΔC_t was calculated by taking the averaged Cq from the RT+NT4 condition and having the RT+ SPTBN1 subtracted from it. The efficacy used for the Pfaffl method is calculated by adding 1.00 to the primer efficacy of GAPDH. The number utilized for the Pfaffl method was calculated by taking the primer and taking it to the power of the ΔC_t .

A)

| Knockdown confirmation SPTBN1 | | | |
|--------------------------------------|--------------|-----------|---------------------|
| Sample SPTBN1 | Wells | Cq | Average (Cq) |
| primers | | | |
| RT+ SPTBN1 | Well 1 | 40.18 | 29.28 |
| knockdown | Well 2 | 29.21 | |
| | Well 3 | 29.35 | |
| RT- SPTBN1 | Well 1 | 38.26 | 36.73 |
| knockdown | Well 2 | 36.12 | |
| | Well 3 | 35.86 | |
| RT+ NT4 knockdown | Well 1 | 27.51 | 26.77 |
| | Well 2 | 26.32 | |
| | Well 3 | 26.49 | |
| RT- NT4 knockdown | Well 1 | 39.09 | 37.46 |
| | Well 2 | 35.86 | |
| | Well 3 | 37.44 | |
| RT+ no siRNA | Well 1 | 26.34 | 26.22 |
| knockdown | Well 2 | 26.10 | |
| | Well 3 | 26.24 | |
| RT- no siRNA | Well 1 | 37.64 | 36.81 |
| knockdown | Well 2 | 36.25 | |
| | Well 3 | 36.54 | |
| H2O sample | Well 1 | 36.51 | 35.27 |
| | Well 2 | 33.81 | |
| | Well 3 | 35.49 | |

B)

| Calculating knockdown of SPTBN1 (Pfaffl method) | | | | |
|--|--------------------|-----------------------------------|-----------------|--------------------------|
| dCt | Eff. SPTBN1 | SPTBN1 | GAPDH | KD SPTBN1 |
| 26.77 - 29.28=-2.51 | 1+1.05=2.05 | 2.05^{-2.51}=0.165 | 0.268944 | 0.165/0.268=0.613 |

Table 5. Confirming Knockdown using GAPDH. GAPDH primers were utilized so a house keeping gene can be analyzed and comparison made to SPTBN1. Each sample had a RT+ and RT- which was used as a control. Each sample condition was done in triplicate and water was used as a negative control. Part A shows the Cq value of each n. The triplicated condition were averaged together. Part B shows the ΔC_t calculation followed by the efficacy used by the Pfaffl method. The ΔC_t was calculated by taking the averaged Cq from the Rt+NT4 condition and having the RT+ SPTBN1 subtracted from it. The efficacy used for the Pfaffl method is calculated by adding 1.00 to the primer efficacy of GAPDH. The number utilized for the Pfaffl method was calculated by taking the primer and taking it to the power of the ΔC_t .

A)

| Knockdown confirmation GAPDH | | | |
|-------------------------------------|--------------|-----------|---------------------|
| Sample GAPDH primers | Wells | Cq | Average (Cq) |
| RT+ SPTBN1 knockdown | Well 1 | 23.78 | 22.78 |
| | Well 2 | 22.37 | |
| | Well 3 | 22.20 | |
| RT- SPTBN1 knockdown | Well 1 | 34.22 | 34.34 |
| | Well 2 | 34.28 | |
| | Well 3 | 34.54 | |
| RT+ NT4 knockdown | Well 1 | 20.49 | 20.48 |
| | Well 2 | 20.57 | |
| | Well 3 | 20.39 | |
| RT- NT4 knockdown | Well 1 | 34.60 | 34.49 |
| | Well 2 | 34.32 | |
| | Well 3 | 34.55 | |
| RT+ no siRNA knockdown | Well 1 | 20.20 | 20.47 |
| | Well 2 | 20.51 | |
| | Well 3 | 20.72 | |
| RT- no siRNA knockdown | Well 1 | 34.24 | 33.98 |
| | Well 2 | 33.65 | |
| | Well 3 | 34.07 | |
| H2O sample | Well 1 | 32.80 | 33.10 |
| | Well 2 | 32.80 | |
| | Well 3 | 33.80 | |

B)

| Calculation for GAPDH sample | | |
|-------------------------------------|------------------------|-----------------------------|
| dCt | Eff. GAPDH | GAPDH |
| 20.48-22.78=-2.30 | 1.00+0.77= 1.77 | 1.77^-2.30= 0.268944 |

Table 6. Infectivity in SPTBN1 Knockdown Cells. Infectivity of HIV in confirmed knockdown cells. SPTBN1 had a decreased expression and the raw infectivity data was the amount of cells that are infected when FACS was conducted. To compare the data was normalized to NT4.

| Raw infectivity data (% infectivity) | | |
|--|---------------|----------|
| SPTBN1 | NT4 (control) | No siRNA |
| 6.00 | 9.61 | 10.48 |
| Normalized infectivity data (% infectivity) | | |
| SPTBN1 | NT4 (control) | No siRNA |
| 62.42 | 100 | 109.06 |

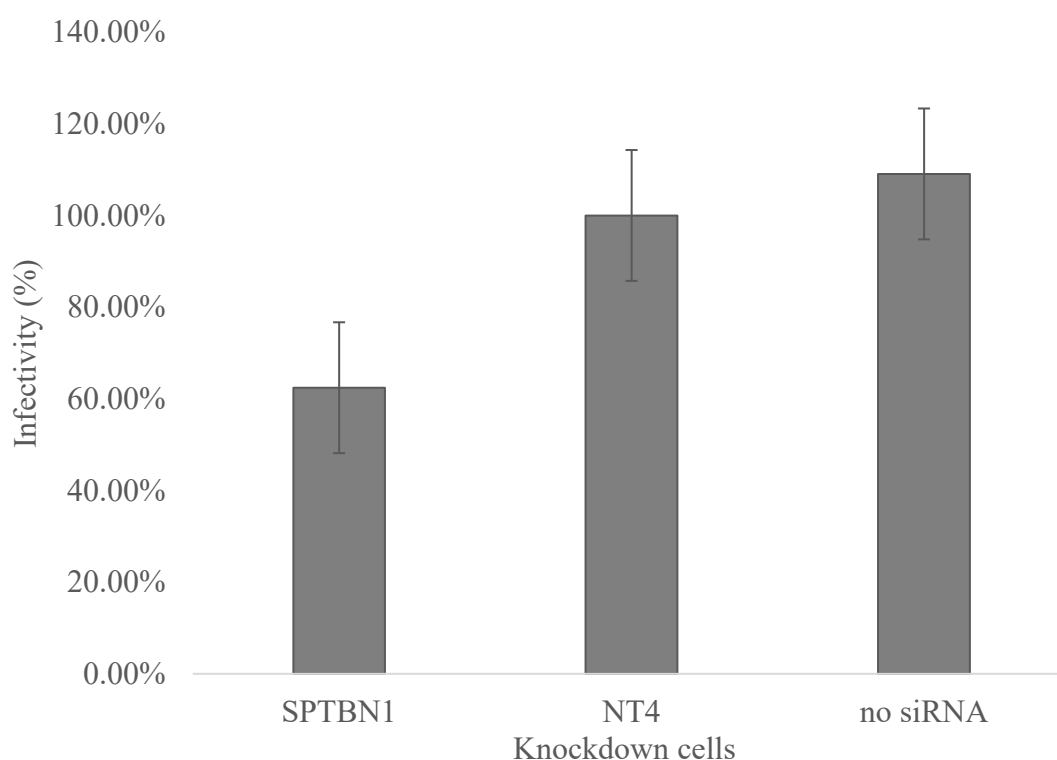


Figure 21. Infectivity with SPTBN1 Knockdown. The graph represents the infectivity of the SPTBN1 knock down to the NT4 control. The data is normalized to NT4. N=1.

Determining the Effect of SPTBN1 Knockdown on Uncoating

Once the knockdown of SPTBN1 was confirmed we proceeded to the second aim of my thesis, which was to determine if the uncoating process of HIV is altered by the down regulation of SPTBN1. To accomplish this, a mini-CsA washout assay was performed (108). This assay works by first having cells that can express TRIM-Cyp. When this protein is expressed, it will bind to the capsid core of HIV and prevent uncoating which leads to a noninfected cell (108). The assay calls for the use of CsA which will be able to bind to TRIM-Cyp and prevent binding to the capsid core of HIV (108). In the presence of CsA uncoating occurs in the cells. When CsA is removed TRIM-Cyp can bind to the remaining cores and prevent uncoating. By removing media that contains CsA at various times post-infection the amount of uncoating that occurs can be found by determining the amount of infectivity at each time point. The infectivity at each time point was then divided by the 5 hr time point (denoted 100%) to get the percent uncoating at each time point. In the CsA washout assay EtOH was used as a carrier control, as EtOH was used to dissolve CsA. In the carrier control, uncoating will not occur and HIV infection will be inhibited.

To determine if early uncoating was affected, CsA was removed at 30 min, 1 hr, and 5 hr post infection. Each of the time points and conditions were done in triplicate for each of the knockdown cells and averaged to obtain the raw data (Table 7A). To calculate the amount of uncoating that took place at each time point, it was assumed that all uncoating took place by the 5 hr time point, based on previous experiments (106). The percent infectivity at each time point (30 min and 1 hr) was then divided by the 5 hr time to give the percent at each time point (Table 7B). The experiment was done in duplicate and the percent uncoating was averaged between these experiments (Table 7C and 7D). At the 30 min time point 19% of the capsid core in the SPTBN1 knockdown sample uncoated, compared 28% in the NT4 control sample and 27% in

the NT4 control (Table 7C and 7D). At 1 hr 34% of the capsid core uncoated in the SPTBN1 knockdown cells, while 58% of the capsid cores uncoated in the NT4 control and 54% of the capsid cores uncoated in the no siRNA control (Table 7C and 7D). In general, there was a decrease in the amount of capsid cores that have uncoated at both time points in the SPTBN1 knockdown cells (Table 7D and Figure 22). There was a decrease of 9% at the 30 min time point and at the 1 hr time point there was 24% decrease in the amount of uncoating in SPTBN1 cells (Figure 22). These results show that the uncoating process was affected by the downregulation of SPTBN1.

Table 7. SPTBN1 Knockdown Affects on Uncoating. The percent of uncoating was obtained from the mini-CSA washout assay. Part A. The raw data of the amount of infectivity obtained in the mini-CSA washout assay at each time point in the various knockdown cell types. Part B. The percentage of the capsid core that have uncoated at each time point. At the 5 hr time point all uncoating should have taken place and will be utilized to obtain the percent of capsid core in other time points. To obtain the amount of uncoating the amount of infectivity at the 30 min and 1 hr time point was divided by the infectivity obtained at the 5 hr time point. Part C. The amount of uncoating at each time point in the various runs. Part D. The averaged amount of uncoating.

A)

| Uncoating data percent of cells infected Sept. 23 2019 | | | |
|--|--------|-------|----------|
| Time point | SPTBN1 | NT4 | No siRNA |
| 30 min | 3.38 | 7.86 | 7.05 |
| 1 hr | 7.35 | 15.68 | 12.05 |
| 5 hr | 29.96 | 37.00 | 33.88 |

B)

| Percent uncoating Sept. 23 2019 | | | |
|---------------------------------|--------|-----|----------|
| Time point | SPTBN1 | NT4 | No siRNA |
| 30 min | 11 | 21 | 21 |
| 1 hr | 25 | 42 | 36 |
| 5 hr | 100 | 100 | 100 |

C)

| Uncoating data (% uncoating) | | | | | | |
|------------------------------|---------------|-----|----------|--------------|-----|----------|
| Time | Sept. 23 2019 | | | Oct. 18 2019 | | |
| | SPTBN1 | NT4 | No siRNA | SPTBN1 | NT4 | No siRNA |
| 30 min | 11 | 21 | 21 | 27 | 36 | 34 |
| 1 hr | 25 | 42 | 36 | 44 | 47 | 72 |
| 5 hr | 100 | 100 | 100 | 100 | 100 | 100 |

D)

| Averaged uncoating data (%uncoating) | | | |
|--------------------------------------|--------|-----|----------|
| Time | SPTBN1 | NT4 | No siRNA |
| 30 min | 19 | 28 | 27 |
| 1 hr | 34 | 58 | 54 |
| 5 hr | 100 | 100 | 100 |

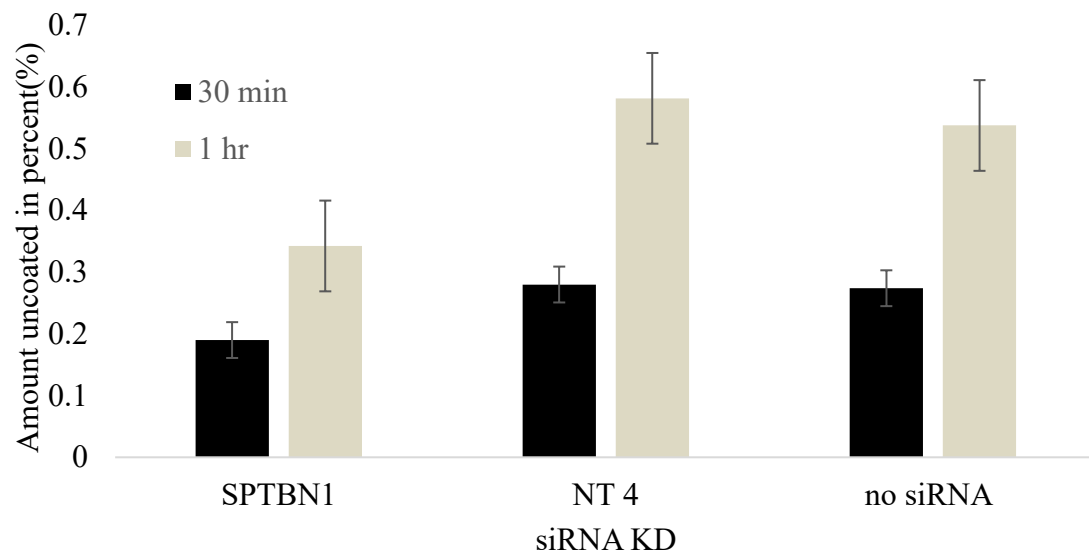


Figure 22. Mini-CsA Washout Assay Bar Graph. The average percent of uncoating at the 30 min and 1 hr after infection is represented in a bar graph. The error bars are the standard error in each sample type. N = 2

DISCUSSION

HIV-1 is a viral agent that leads to the development of AIDS and eventual death in patients (1). Therapies exist to control HIV-1 replication, but due to the rapid mutation rate of HIV-1 and lack of adherence to medication, ART drugs can become ineffective (72). HIV strains that are resistant to ART make treating patients difficult and can cause the patient to progress quickly into AIDS. Some limitation of ART therapy includes the inability to target viral revivor especial in the CNS which is due to the highly selective nature the BBB (54). The BBB is made up of astrocytes and cells responsible for the immune response in the CNS are microglial cells (54). When microglial cells become infected with HIV, they cause inflammation to occur (58). The inflammation leads to the symptoms of HAD/HAND. The inability to target microglial cells leads to a viral revivor to form in the CNS, inflammation to occur, and leads to the formation of HAND/HAD. Other therapies are needed to assist with controlling HIV replication and reducing the incidence of HAD/HAND. Host factors are an area of research that holds the possibility of assisting ART therapies. Targeting host factors with other medication or other processes can help control the low levels of HIV-1 virions being produced and can reduce the level of virion formation in viral revivors in the CNS. Investigating the role host factors play in HIV infection will lead to a better understanding of the infection process which could lead to better therapies or a cure to HIV-1 (8, 15, 16).

SPTBN1 is a host factor which holds the possibly of reducing HIV-1 replication (8, 15, 16). SPTBN1 is involved with structural support and organization of the actin cytoskeleton (9, 90). SPTBN1 was also shown to bind to the capsid core of HIV-1 (8). However, further experimentation of SPTBN1 interaction with HIV-1 was not investigated, the goal of my thesis

was to better understand how SPTBN1 interacts with HIV-1 infection. The hope was to not only gain more information about host factor and viral interaction but pinpoint the exact role SPTBN1 plays in the infection process.

The first aim of my thesis was to investigate the infectivity of HIV when SPTBN1 is downregulated. When SPTBN1 is downregulated the infectivity of HIV should decrease in TCN14 cells. This aim was accomplished by first downregulating SPTBN1. To confirm SPTBN1 knockdown, qRT-PCR was utilized, and data analyzed using the Pfaffl method, which allows comparisons to be made based on the expression of a housekeeping gene (GAPDH) and a target gene (SPTBN1). This method controls for the different number of cells in each sample set and the primer efficiency for each gene. To start confirming knockdown, the annealing temperature for each primer set was determined by qPCR and the optimal temperature for both primer sets was found to be 60°C (Figure 17). The primer efficiency for SPTBN1 was 1.05 and for GAPDH primers efficacy was 0.77 (Table 2 and 3; Figure 19 and 20). The primer efficiency was determined so that we could obtain the ΔC_t of the experimental group. To confirm knockdown of SPTBN1, RNA was extracted from TCN14 cells that were transfected with siRNA (SPTBN1, NT4, or no siRNA). Quantitative RT-PCR was performed to determine the expression level of SPTBN1 and GAPDH in each knockdown sample. SPTBN1 was knocked down 39.70% in the SPTBN1 siRNA samples (Table 7).

After confirming SPTBN1 was knocked down in the microglial cell experiential group, HIV infectivity was tested. TCN14 cells were transfected with pools of siRNAs targeting SPTBN1, or control nontargeting RNA and infected with HIV-GFP. The number of infected cells in each experimental condition was obtained by a flow cytometer and was done in duplicate. Each run was then averaged together and normalized to the NT4 control. In these

experiments the infectivity of HIV-GFP was decreased by 19.75% in SPTBN1 knockdown cells, when compared to the control cells (Table 1; Figure 16). This result showed that SPTBN1 plays a role in HIV-1 infection in TCN14 cells. However, the role SPTBN1 plays in the infection process is still unknown.

The results obtained from Aim 1 correlated with what was obtained from three previous publications. In the Gallo publication SPTBN1 knockdown correlated to a decrease in HIV infectivity when wild type and VSV-g pseudotyped HIV was utilized (15). However, there was a difference seen in the infectivity between viral types. When knockdown cells were infected with WT HIV there was a decrease of about 60%, when cells were infected with VSV-g HIV there was a decrease between 20-40%. This is in line with my result which showed a decrease of 19.75% when TCN14 cells were infected with VSVg-HIV-GFP.

Previous publications saw a difference in the infectivity between viral types which points to a possibility of SPTBN1 playing a role in the uncoating process of HIV. The Dai publication showed that when monocytes are differentiated into macrophages by IL-27 it decreased the expression of SPTBN1 which correlated to a decreased infectivity (8). The amount of decrease seen in the differentiated monocytes was 80% when compared to the control. The publication also demonstrated that when SPTBN1 was down regulated it caused an alteration in the actin cytoskeleton which not only affected the infectivity of HIV-1, but HSV-2 and influenza. Finally, the Brass publication depicted that SPTBN1 could play a role in uncoating along with other processes of infection (16). The decrease in infectivity in the publication was 24% which was similar to my result. My results and other publications show that the downregulation of SPTBN1 correlates to decreased infectivity of HIV. However, the exact role SPTBN1 plays in the infection process is still unknown but could be involved fusion, uncoating or viral trafficking of

HIV. The Dai publication however did demonstrate that SPTBN1 can bind to the capsid core of HIV and interact with the actin cytoskeleton which somehow facilitates infection. SPTBN1 interaction with the capsid core suggests that one likely role it plays in the infection process is uncoating. Aim 2 of my thesis was to see if SPTBN1 plays a role in the uncoating process.

In Aim 2, I sought to determine the uncoating rate in SPTBN1 knockdown cells. A mini-CsA washout assay was performed on transfected cells to measure the uncoating process over time in control and SPTBN1 knockdown cells. The CsA-washout assay is based on removal of media which contains CsA (108). By removing CsA, uncoating is halted, which will also affect the infectivity (108). The CsA media was removed at various time points (30 min, 1 hr, 5 hr) and the percent of uncoating was obtained by taking the amount of infectivity at 30 min and 1 hr then dividing it by the infectivity at the 5 hr time point. At the 30 min time point, uncoating was inhibited by 9% and at the 1 hr time point uncoating was inhibited by 24% in the SPTBN1 knockdown cells when compared to the control (Table 7; Figure 22). The data obtained from the mini-CsA washout assay shows that there is a decrease in the amount of uncoating when SPTBN1 was downregulated and that SPTBN1 plays a role in uncoating.

SPTBN1 plays a role in uncoating by decreasing the amount of capsid cores that have uncoated and the amount of infectivity when SPTBN1 was down regulated. This information adds to the knowledge of host factor interaction with HIV infection. However, much more research is needed to denote how SPTBN1 participates in other processes of HIV regulation and how the downregulation of SPTBN1 affects later time points (2-6 hr) of uncoating. Since the stability of the capsid cores varies between virions, testing at the later time points allows me to have a better understanding of how the downregulation of SPTBN1 will affect uncoating kinetics in

TCN14 cells and if the decrease seen in the early time points will carry over in the later time points.

When altering the replication process of HIV, it will lead to a change in infectivity. As the results showed, decreasing the amount of uncoating that occurs leads to a decrease in infectivity. There was only a decrease of 19.75% when the infectivity was assessed in SPTBN1 knockdown cells (Figure 16). The decrease in infectivity correlated with a 9% decrease in uncoating at 30 min and a 24% decrease at 1 hr (Figure 22). The downregulation of SPTBN1 plays a role in uncoating however, other factors may be at work that affect infectivity, including fusion and viral trafficking. SPTBN1 might participate in fusion of the viral and host membranes due to this process reliance on the actin cytoskeleton. Evidence that fusion can be affected is seen in the different ways WT and VSV-g HIV gain entry to the cell. WT enters the cell via fusion and VSV-g gains access by endocytosis. When the Gallo publication assessed the infectivity in both viral types there was a decrease in both, however there was more of a decrease seen in the WT virus. Since the only difference in the replication cycle of WT and VSV-g virus is fusion, this needs to be accessed to understand why there is a difference and does SPTBN1 play a role in this replicative step. Viral trafficking might also be affected. While capsid cores rely more on microtubules for transport to the nucleus, the actin cytoskeleton might act as an alternative transport pathway when other paths are blocked.

Aim 3 of my thesis was to investigate if SPTBN1 is associated or participates in the fusion process of HIV. However, due to COVID-19 related regulations and hardships I was unable to evaluate this process and the role SPTBN1 plays in fusion. To test the fusion process of HIV-1 a kinetic fusion assay would have been performed. This assay works by inserting a dye that has a beta lactam ring into the cells and subsequently infect the cell with a HIV virus that

has a beta lactamase in the virion. Once the cell is infected with the HIV- beta lactamase virus the dye will change color and by taking samples at various time point we can see if the down regulation of SPTBN1 affects fusion of HIV. When SPTBN1 is downregulated in the TCN14 cells the amount of fusion will also decrease.

Future Directions and Optimizing Knockdown

In my thesis knowledge has been gained about the role SPTBN1 plays in the infection process. However, much remains unknown regarding SPTBN1 participation in other replication steps of HIV-1. One question which needs to be answered is weather further knockdown of SPTBN1 will increase the affects in the infectivity and uncoating assays. I obtained a knockdown of 39.75% when SPTBN1 was downregulated in TCN14 cells. My goal will be to obtain 80% knockdown which is seen in the Dai publication (8). I can optimize siRNA knockdown by changing the siRNA utilized or the transfection protocol. A more complete knockdown may yield more information about the role SPTBN1 plays in uncoating, fusion, and viral trafficking of HIV-1 (8, 15, 16).

Here, I performed a mini-CsA washout assay, but a full CsA-uncoating assay needs to be conducted. The full CsA-washout assay will test uncoating at time points starting at 0 hr up to 6 hr which is different than the mini-CsA washout assays which only tested uncoating at the 30 min and 1 hr time point. The full CsA washout assays will show if the decrease in uncoating already seen in the early time points will carry over to the later time points of uncoating. The full CsA washout assay will give us a better understanding of how SPTBN1 plays a role in uncoating and how its downregulation affects uncoating kinetics.

Since fusion relies on the actin cytoskeleton and SPTBN1 has a direct role in the actin cytoskeleton, fusion is another important replication process which SPTBN1 could affect HIV infectivity. A fusion assay in the knockdown will tell me if uncoating is truly affected or if the decrease seen was due to fusion being affected which led to altered uncoating. The evidence for this is seen in the infectivity difference between the WT HIV and VSV-g HIV in the Gallo publication. The two viruses enter the cell via different mechanism which points to SPTBN1 playing a role in fusion. Fusion experiments will need to be carry out with WT HIV and VSV-g HIV which are virus that have different entry pathways fusion and endocytosis, respectively. This will be done by a Blam fusion assay and a kinetic fusion assay. This experiment will demonstrate if SPTBN1 is involved in fusion and if there is a difference between the two virus types. This could lead to new viral targets associated with the fusion process that could be targeted for therapeutics and reduce the amount of viral replication which could decrease the incident of HAD/HAND.

The last replication process where SPTBN1 can play a role is viral trafficking. The actin cytoskeleton can play a role in multiple steps of the replication process (9, 70, 75, 104). However, microtubules are responsible for the majority of capsid core being trafficked to the nucleus. Infectivity of HIV-1 was decreased when SPTBN1 was down regulated along with an alteration in the actin cytoskeleton which affected not only HIV-1 and other viruses. Actin could act as an alternative pathway to traffic capsid cores, making actin and SPTBN1 one pathway that might traffic the virus from the membrane to the nucleus.

The final question which needs to be answered is how microglial cells respond to IL-27. The Dai publication showed that when macrophages were stimulated with IL-27, SPTBN1 was decreased which led to a decrease in HIV infectivity. By testing TCN14 cells response to IL-27 it

will show if this interleukin can be used as a therapy to control HIV-1 infection but also allow for a better understand the role host factors plays in HIV infection. To test how IL-27 will affect TCN14 cells, the cells will be stimulated with IL-27 which is in the media and the expression of SPTBN1 will be determined by qRT-PCR. For the control, CSF will be utilized and should not affect the expression of SPTBN1.

From my data, there remains room to increase the amount of knockdown of SPTBN1 in TCN14 cells. There was only a 39% decrease in SPTBN1 expression, by increase the amount of knockdown this will hopefully further decrease the infectivity and the amount of uncoated capsid cores. There are multiple ways to increase the amount of knockdown including trying other transfection agents, such as lipofectamine 3000 from ThermoFisher or HiPerFect Transfection Reagent from Qiagen. Another item which can be change is trying a new set of siRNA which target different sequences within SPTBN1, or we can use a short hairpin RNA instead of fully processed siRNAs. Another way to possibly knockdown SPTBN1 is with IL-27, similar to the Dai publication (8). However, it is unknown if SPTBN1 can be downregulated by IL-27 in TCN14 cells and how much of an affect it will have. A complete knockout cell line could be made by using CRISPR or shRNA and used to determine the role SPTBN1 plays in the infection process of HIV-1. However, it is unknown how a complete knockout of SPTBN1 will affect the physiology of the cell due to its interaction with actin cytoskeleton. The actin cytoskeleton is an intricate part of the cell, and it remains unknown how TCN14 cells will respond, which could lead to death of the cell line. With the increased amount of knockdown there will be a further decrease in infectivity along with a greater effect on uncoating.

Full CsA Washout and Fusion Assay

The goal of the full CsA washout assay is to test whether the later time points of uncoating are affected by SPTBN1 knockdown. The full CsA-washout assay follows the same principle of the mini-CsA washout assay and will be carried out in the same manner (108). The difference between the mini and the full CsA washout assays is that more time points will be added to include 15 min, 45 min, 2 hr, 3 hr, 4 hr and 6 hr time points in the assay. This will yield more information about the kinetics of uncoating when SPTBN1 is downregulated (108). To obtain the percent uncoating, the amount of infectivity at time points will be divided by the infectivity at the 6 hr instead of the 5 hr time point in the mini-CsA-washout assay. Since SPTBN1 plays a role in the early time points of uncoating it is likely the later time points of uncoating are affected as well. This will allow me to determine the full involvement of SPTBN1 in the uncoating process and if uncoating is delayed.

Since the uncoating process is affected, the next process that needs to be investigated is viral fusion. Since fusion proceeds uncoating this process need to be investigated to make sure that the affects seen in uncoating are not due to altered fusion. There are two assays to test the fusion process: The BlaM assay and the fusion kinetic assay (109). The BlaM assay consists of a one-time measurement of fusion, which will tell me if the process is affected, but nothing about whether the kinetics of the process is affected (109). The kinetic fusion assay allows for multiple measurements of fusion to be taken over time, yielding more information about the timing of fusion and any alterations.

A BlaM assay should be conducted first to see if the process is altered. The BlaM assay uses a kit which is commercially available. The principle behind the assay is that fusion is tracked by a color change in a dye (109). The dye (CCF2-AM) contains a beta lactam ring and emits a green light when it is un-cleaved. Once the beta lactam ring is cleaved the dye will emit a

blue light (109). The dye is inserted in the cell and infected with HIV which contains a beta lactamase attached to the viral accessory protein Vpr (109). When HIV fuses with the cell, Vpr with the lactamase attached is released into the cell, comes in-contact with the dye and causes the change in color (109). The color change can be detected by flow cytometry and based on the emission of the various colors of light the amount of fusion can be determined (109).

To start the BlaM assay TCN14 cells will be grown, transferred to a 6-well plate, and transfected with siRNA (SPTBN1, NT4, or no siRNA). The day after transfection, cells are transferred to a 96-well plate and CCF2-AM dye which is in the media is inserted into the cells due its highly lipophilic nature. Probenecid can be used to help load the dye into the cells if necessary. After the dye is inserted, infection occurs with HIV-Vpr lac and cells are preserved. Flow cytometry is used to detect the amount of cells that changed from green to blue light, and therefore the amount of fusion. If the BlaM assay shows an alteration of fusion by SPTBN1 knock down, then a kinetic assay will be performed. The fusion kinetic assay is started and conducted the same manner to the BlaM assay, however, multiple samples are fixed at various time points after the TCN14 cells are infected and the fusion process is occurring. The time point will include 15 min, 30 min, 1 hr, 2 hr and 4 hr time points. The results will allow fusion to be tracked over time to determine how SPTBN1 affects fusion kinetics. If fusion is affected more investigation will need to occur to see if SPTBN1 plays a role in both fusion and uncoating or one or the other which could lead me to rethink how SPTBN1 participates in HIV infection.

WT HIV and VSV-g-HIV-GFP Differences

Another discrepancy that needs to be evaluated is the role that SPTBN1 plays in WT-HIV and VSV-g HIV. The Gallo publication demonstrated a difference in the amount of infectivity

between the two viral types, wild type HIV and VSV-g HIV in HeLa cells when SPTBN1 was downregulated. The publication speculated that fusion is the most likely candidate for the discrepancy between SPTBN1 knockdown on the two viral types (15). One speculation on why there was a difference between viral types and but could be because of the way the virus enters the cell and the reliance on the actin cytoskeleton between the two.

To deduce possible differences in fusion between the two HIV strains, BlaM and the kinetic fusion assays will be performed on both the WT-HIV and VSV-g HIV. This will allow me to make a comparison between the two virus and see how big of a role SPTBN1 plays in each. Due to limited biohazard protocols at Missouri State University and the risk of working with replication competent HIV virus, this experiment would need to be conducted at or by a collaborator's laboratory. Testing fusion will allow comparison of the modes of entry between WT-HIV and VSV-g HIV. Moreover, using SPTBN1 knockdown, we can see if SPTBN1 plays a role in each. If fusion is affected by the down regulation of SPTBN1, it allows for better interpretation of the uncoating result and give more details about the role SPTBN1 plays in the infection process. After fusion of the two virus types there is no difference in the later process of infection, uncoating and viral trafficking are the same between the two viruses. If there is a difference between the viral types in the infectivity in TCN14 cells, this assay will demonstrate it is due to fusion. If a difference between the two viruses exist, it could be due to more of a dependence on the actin cytoskeleton in the fusion process of WT-HIV (9). Since both viral types are widely used in many research labs it is important to denote why there is a difference and how the two viral types depend on the actin cytoskeleton.

Viral Trafficking and TCN14 Cells Response to IL-27

Another important replication process which needs to be evaluated is HIV-1 trafficking. In the Dai publication it was shown that the actin cytoskeleton arrangement was altered when SPTBN1 was downregulated, which correlated to decreased infectivity. In the same publication the infectivity of Herpes simplex 2 and influenza followed the same trend (8). This could be due to fusion or trafficking of the various viruses. Since the viruses must migrate to the nucleus as part of their replication process, viral trafficking could be a possible source for the decreased infectivity. Migration of HIV-1 capsid cores relies heavily on the microtubule system of the cell, but the actin cytoskeleton could be utilized as an alternative pathway (71). This could be why there was not a drastic decrease in the amount of infectivity in my data. Regardless, SPTBN1 role in trafficking needs to be explored.

There are many assays available to track the movement of viral particles all of which involve three basic steps: particle detection/tracking, trajectory classification, and physical modeling (110). The easiest way to track, visualize viral progression, and map the trajectory is to fluorescently label capsid cores and utilize microscopy. The process can be performed by infecting cells with double labeled virus and visualization of the fluorescent signal by light microscopy (110). The double label HIV virus has two different signals, the outer membrane labeled with S15-cherry and the capsid core is labeled with GFP by inserting the protein between the matrix and the capsid protein (110). Utilization of this virus will not only allow me to track the movement of the virus but denote what replication process the virus is using. Before HIV-1 enters the cells, the virus will have a red signal. Once HIV enters the cell via endocytosis (VSVg-HIV) and fuses with the cell membrane, the red signal dissipates and only the green-fluorescent signal remains. The green fluorescence illuminates for the capsid core, and the migration can then be tracked through the cells. Once the GFP signal dissipates the virus has uncoated. The dissipation of the GFP signal will be lost when the capsid core breaks apart. By utilizing the double labeled virus, it will allow me to visualize how the

capsid core migrates in the cells and tell me if SPTBN1 plays a role in viral trafficking. A fluorescent trafficking assay should be started by first transfecting TCN14-cells with a siRNA (SPTBN1, NT4, or no siRNA). After the cells are transfected, they are moved to a 24-well plate with a glass cover slip that are treated to allow cells to adhere and then infect with the double labeled virus by spinoculation. At time point zero, 15 min, 30 min, 1 hr, 2 hr, 3 hr, 4 hr, 5 hr and 6 hr, the cells will be fixed. The number of capsid cores that are intact, and the distance away from the cell membrane will be compared between SPTBN1 knockdown and control cells at each time point. Since the downregulation of SPTBN1 alters the actin cytoskeleton I believe there would be a decrease in the amount of capsid cores trafficked to the nucleus of the cell.

Another vital area which needs to be explored is to determine if SPTBN1 is downregulated in response to IL-27. This will not only determine if IL-27 can downregulate SPTBN1 and can be utilized as a therapeutic agent, but this process also holds the possibility of knocking down SPTBN1 other than the utilization of a siRNA. To start the experiment, cells will be grown in three separate media conditions (CHME3 media, M-CSF as a control, and IL-27) which is added to growth media and incubated for 24 hrs. After the incubation period RNA will be extracted and RT-qPCR will be carried out to determine the amount of knockdown. GAPDH will be utilized as a housekeeping gene so that the expression of SPTBN1 can be compared and the amount of knockdown determined. Since macrophages are affected by IL-27 and decrease the amount of SPTBN1, I believe TCN14 cells will have a similar response and have a decreased amount of SPTBN1 expression.

In the Dai publication IL-27 was able to decrease SPTBN1 when monocytes were differentiated into macrophages which was done without affecting the physiology of the cells (8). However, it is unknown if IL-27 stimulated TCN14 cells will have altered physiology or have

any affect at all. If IL-27 can affect TCN14 cells and decrease SPTBN1 expression, then the physiology of the cell will need to be investigated. To investigate the physiological response, IL-27 stimulated TCN14 cells will be examined by determining receptor expression, phagocytosis ability, response to chemotaxis agents and the ability to mount an immune response (8). To start the various experiments, TCN14 cells will be grown in a 10 cm dish until 100% confluent at which point the cells will be split and placed in a 6-well plate by the procedure described in the method section. The TCN14 cells in the 6-well plate will be seeded at 0.7×10^6 cells/well and grown in CHME3 media that include IL-27, M-CFS and regular CHME3 (8). The cells will incubate for 24 hr to allow the cells to respond to the various media components. After the incubation period the phagocytic ability of the cell will be tested by the *E. coli* bioparticle phagocytosis kit (8). To utilize the kit 1.0×10^6 TCN14 cells will be incubated with 20 μ l of *E. coli* particles for 30 min at 37°C. A negative control will be placed on ice to prevent TCN14 cells from phagocytosing the *E. coli* particles (8). After the 30 min incubation period cells will be washed and the amount of phagocytosis will be analyzed by flow cytometry.

If IL-27 affects TCN14 cells, then the response to chemotactic agents by the stimulated TCN14 cells will also be investigated. To analyze the chemotactic ability of TCN14 cells, the cells will be stimulated with IL-27 as previously described. After the TCN14 cells have been stimulated they are seeded in a 48-well plate and the migration tested by the R&D system (8). The R&D system consists of a 48-well micro-chemotaxis plate which was developed by Falk in the 1980's (111). TCN14 cells will be placed in the 48-well plate in the presents of SDF-1 α and RANTES. Both SDF-1 α and RANTES are chemotaxis agents which can cause migration of immune cells. Once the cells are seeded in the plate, the ability of TCN14 cell to migrate across the plate in response to the chemotaxis agent will be determine by microscopy. The data will be

presented as the number of cells per high power field which will allow the determination if the physiology of TCN14 cells are affected by IL-27 stimulation. If IL-27 is able to down regulate SPBTN1, I believe that the physiology of the cells will be unaffected, and the stimulated cells will have the same response as the control cells.

To test the ability of TCN14 cells to mount an immune response when stimulated with IL-27, the production of cytokines will be analyzed by the Milliplex assay kit (8). The assay is commercially available and can determine the amount of production of various interleukins to include IL-1 β , IL-5, IL-6, IL-12 β , IL-13, IL-17, CSF3, Fractalkine, TGF α , IL-2R α (8). To start the experiment TCN14 cells will be grown and stimulated with IL-27 by the previously mentioned procedure. After the cells were grown and the 2-day incubation period has past, the supernatant will be analyzed to determine the cells ability to mount an immune response. The Milliplex assay will be performed on the supernatant following the manufacture's recommendation. By determining the immune response produced by IL-27, a determination can be made if this interleukin can be utilized as a therapeutic agent for HIV-1.

By conducting a fusion assay, a full CsA-washout assay, and the viral trafficking experiments, we will have a better understanding of the role SPTBN1 plays in not only WT-HIV, but VSV-g HIV replication processes in TCN14 cells. The better understanding of how host factors participate in HIV infection will hopefully lead to future therapeutics or a cure for HIV-1, These targets include host factor and interleukins that can control the expression of various host factors. By altering host factor interaction with HIV proteins, we will hopefully reduce the incident of HAD/HAND, have other means of treating resistant strains of HIV, and hopefully reduce the amount of HIV particles in viral reservoirs. The utilization of therapeutics involving host factors will lead to better outcomes and prolonged life for HIV-1 patients.

REFERENCES

1. Freed EO. 2001. HIV-1 replication. *Somat Cell Mol Genet* 26:13–33.
2. 1990. HIV/AIDS Surveillance. U.S. Department of Health and Human Services, Public Health Service, Centers for Disease Control, Center for Infectious Diseases, Division of HIV/AIDS.
3. Meriki HD, Tufon KA, Anong DN, Atanga PN, Anyangwe IA, Cho-Ngwa F, Nkuo-Akenji T. 2019. Genetic diversity and antiretroviral resistance-associated mutation profile of treated and naive HIV-1 infected patients from the Northwest and Southwest regions of Cameroon. *PLoS One* 14:e0225575.
4. Okoye AA, Picker LJ. 2013. CD4(+) T-cell depletion in HIV infection: mechanisms of immunological failure. *Immunol Rev* 254:54–64.
5. Campbell EM, Hope TJ. 2015. HIV-1 capsid: the multifaceted key player in HIV-1 infection. *Nat Rev Microbiol* 13:471–483.
6. Lopez-Galindez C, Pernas M, Casado C, Olivares I, Lorenzo-Redondo R. 2019. Elite controllers and lessons learned for HIV-1 cure. *Curr Opin Virol* 38:31–36.
7. Korber B, Muldoon M, Theiler J, Gao F, Gupta R, Lapedes A, Hahn BH, Wolinsky S, Bhattacharya T. 2000. Timing the ancestor of the HIV-1 pandemic strains. *Science* 288:1789–1796.
8. Dai L, Lidie KB, Chen Q, Adelsberger JW, Zheng X, Huang D, Yang J, Lempicki RA, Rehman T, Dewar RL, Wang Y, Hornung RL, Canizales KA, Lockett SJ, Lane HC, Imamichi T. 2013. IL-27 inhibits HIV-1 infection in human macrophages by down-regulating host factor SPTBN1 during monocyte to macrophage differentiation. *J Exp Med* 210:517–534.
9. Ospina Stella A, Turville S. 2018. All-Round Manipulation of the Actin Cytoskeleton by HIV. *Viruses* 10.
10. Colomer-Lluch M, Ruiz A, Moris A, Prado JG. 2018. Restriction Factors: From Intrinsic Viral Restriction to Shaping Cellular Immunity Against HIV-1. *Frontiers in Immunology*.
11. Cenker JJ, Stultz RD, McDonald D. 2017. Brain Microglial Cells Are Highly Susceptible to HIV-1 Infection and Spread. *AIDS Res Hum Retroviruses* 33:1155–1165.
12. Delaney MK, Malikov V, Chai Q, Zhao G, Naghavi MH. 2017. Distinct functions of diaphanous-related formins regulate HIV-1 uncoating and transport. *Proc Natl Acad Sci U S A* 114:E6932–E6941.
13. Clifford DB, Ances BM. 2013. HIV-associated neurocognitive disorder. *Lancet Infect Dis* 13:976–986.

14. Zhen A, Rezek V, Youn C, Lam B, Chang N, Rick J, Carrillo M, Martin H, Kasparian S, Syed P, Rice N, Brooks DG, Kitchen SG. 2017. Targeting type I interferon-mediated activation restores immune function in chronic HIV infection. *J Clin Invest* 127:260–268.
15. Gallo DE, Hope TJ. 2012. Knockdown of MAP4 and DNAL1 produces a post-fusion and pre-nuclear translocation impairment in HIV-1 replication. *Virology* 422:13–21.
16. Brass AL, Dykxhoorn DM, Benita Y, Yan N, Engelman A, Xavier RJ, Lieberman J, Elledge SJ. 2008. Identification of Host Proteins Required for HIV Infection Through a Functional Genomic Screen. *Science*.
17. Scully EP, Lockhart A, Garcia-Beltran W, Palmer CD, Musante C, Rosenberg E, Allen TM, Chang JJ, Bosch RJ, Altfeld M. 2016. Innate immune reconstitution with suppression of HIV-1. *JCI Insight* 1:e85433.
18. Gougeon M-L, -L. Gougeon M. 2017. Alarmins and central nervous system inflammation in HIV-associated neurological disorders. *Journal of Internal Medicine*.
19. Edén A, Marcotte TD, Heaton RK, Nilsson S, Zetterberg H, Fuchs D, Franklin D, Price RW, Grant I, Letendre SL, Gisslén M. 2016. Increased Intrathecal Immune Activation in Virally Suppressed HIV-1 Infected Patients with Neurocognitive Impairment. *PLoS One* 11:e0157160.
20. Gangwani MR, Kumar A. 2015. Multiple protein kinases via activation of transcription factors NF- κ B, AP-1 and C/EBP- δ regulate the IL-6/IL-8 production by HIV-1 Vpr in astrocytes. *PLoS One* 10:e0135633.
21. da Fonseca ACC, Matias D, Garcia C, Amaral R, Geraldo LH, Freitas C, Lima FRS. 2014. The impact of microglial activation on blood-brain barrier in brain diseases. *Front Cell Neurosci* 8:362.
22. Garcia-Mesa Y, Jay TR, Checkley MA, Luttge B, Dobrowolski C, Valadkhan S, Landreth GE, Karn J, Alvarez-Carbonell D. 2017. Immortalization of primary microglia: a new platform to study HIV regulation in the central nervous system. *J Neurovirol* 23:47–66.
23. Xu JP, Francis AC, Meuser ME, Mankowski M, Ptak RG, Rashad AA, Melikyan GB, Cocklin S. 2018. Exploring Modifications of an HIV-1 Capsid Inhibitor: Design, Synthesis, and Mechanism of Action. *Q J Crude Drug Res* 5.
24. Poudyal D, Yang J, Chen Q, Goswami S, Adelsberger JW, Das S, Herman A, Hornung RL, Andresson T, Imamichi T. 2019. IL-27 posttranslationally regulates Y-box binding protein-1 to inhibit HIV-1 replication in human CD4⁺ T cells. *AIDS* 33:1819–1830.
25. Chevalier MF, Didier C, Girard P-M, Manea ME, Campa P, Barré-Sinoussi F, Scott-Algara D, Weiss L. 2016. CD4 T-Cell Responses in Primary HIV Infection: Interrelationship with Immune Activation and Virus Burden. *Front Immunol* 7:395.

26. Mamik MK, Ghorpade A. 2014. Chemokine CXCL8 promotes HIV-1 replication in human monocyte-derived macrophages and primary microglia via nuclear factor- κ B pathway. *PLoS One* 9:e92145.
27. Chen Q, Swaminathan S, Yang D, Dai L, Sui H, Yang J, Hornung RL, Wang Y, Huang DW, Hu X, Lempicki RA, Imamichi T. 2013. Interleukin-27 is a potent inhibitor of cis HIV-1 replication in monocyte-derived dendritic cells via a type I interferon-independent pathway. *PLoS One* 8:e59194.
28. Serramía MJ, Jesús Serramía M, Ángeles Muñoz-Fernández M, Álvarez S. 2016. HIV-1 increases TLR responses in human primary astrocytes. *Scientific Reports*.
29. Borges ÁH, O'Connor JL, Phillips AN, Rönsholt FF, Pett S, Vjecha MJ, French MA, Lundgren JD. 2015. Factors Associated With Plasma IL-6 Levels During HIV Infection. *Journal of Infectious Diseases*.
30. de Medeiros RM, Valverde-Villegas JM, Junqueira DM, Gräf T, Lindenau JD, de Mello MG, Vianna P, Almeida SEM, Chies JAB. 2016. Rapid and Slow Progressors Show Increased IL-6 and IL-10 Levels in the Pre-AIDS Stage of HIV Infection. *PLoS One* 11:e0156163.
31. Oguariri RM, Dai L, Adelsberger JW, Rupert A, Stevens R, Yang J, Huang D, Lempicki RA, Zhou M, Baseler MW, Clifford Lane H, Imamichi T. 2013. Interleukin-2 Inhibits HIV-1 Replication in Some Human T Cell Lymphotropic Virus-1-infected Cell Lines via the Induction and Incorporation of APOBEC3G into the Virion. *Journal of Biological Chemistry*.
32. Swaminathan S, Qiu J, Rupert AW, Hu Z, Higgins J, Dewar RL, Stevens R, Rehm CA, Metcalf JA, Sherman BT, Baseler MW, Lane HC, Imamichi T. 2016. Interleukin-15 (IL-15) Strongly Correlates with Increasing HIV-1 Viremia and Markers of Inflammation. *PLoS One* 11:e0167091.
33. Fernandes SM, Pires AR, Ferreira C, Foxall RB, Rino J, Santos C, Correia L, Poças J, Veiga-Fernandes H, Sousa AE. 2014. Enteric Mucosa Integrity in the Presence of a Preserved Innate Interleukin 22 Compartment in HIV Type 1–Treated Individuals. *J Infect Dis* 210:630–640.
34. Højen JF, Rasmussen TA, Andersen KLD, Winckelmann AA, Laursen RR, Gunst JD, Møller HJ, Fujita M, Østergaard L, Søgaard OS, Dinarello CA, Tolstrup M. 2015. Interleukin-37 Expression Is Increased in Chronic HIV-1-Infected Individuals and Is Associated with Inflammation and the Size of the Total Viral Reservoir. *Mol Med* 21:337–345.
35. Garg A, Rawat P, Spector SA. 2015. Interleukin 23 Produced by Myeloid Dendritic Cells Contributes to T-Cell Dysfunction in HIV Type 1 Infection by Inducing SOCS1 Expression. *The Journal of Infectious Diseases*.

36. Stone K, Woods E, Szmania SM, Stephens OW, Garg TK, Barlogie B, Shaughnessy JD Jr, Hall B, Reddy M, Hoering A, Hansen E, van Rhee F. 2013. Interleukin-6 receptor polymorphism is prevalent in HIV-negative Castleman Disease and is associated with increased soluble interleukin-6 receptor levels. *PLoS One* 8:e54610.
37. Shive CL, Mudd JC, Funderburg NT, Sieg SF, Kyi B, Bazdar DA, Mangioni D, Gori A, Jacobson JM, Brooks AD, Hardacre J, Ammori J, Estes JD, Schacker TW, Rodriguez B, Lederman MM. 2014. Inflammatory Cytokines Drive CD4 T-Cell Cycling and Impaired Responsiveness to Interleukin 7: Implications for Immune Failure in HIV Disease. *The Journal of Infectious Diseases*.
38. Gangwani MR, Kumar A. 2015. Multiple Protein Kinases via Activation of Transcription Factors NF- κ B, AP-1 and C/EBP- δ Regulate the IL-6/IL-8 Production by HIV-1 Vpr in Astrocytes. *PLOS ONE*.
39. Henrick BM, Yao X-D, Zahoor MA, Abimiku A 'le, Osawe S, Rosenthal KL. 2019. TLR10 Senses HIV-1 Proteins and Significantly Enhances HIV-1 Infection. *Front Immunol* 10:482.
40. Alvarez-Carbonell D, Garcia-Mesa Y, Milne S, Das B, Dobrowolski C, Rojas R, Karn J. 2017. Toll-like receptor 3 activation selectively reverses HIV latency in microglial cells. *Retrovirology* 14:9.
41. Williams LD, Amatya N, Bansal A, Sabbaj S, Heath SL, Sereti I, Goepfert PA. 2014. Immune activation is associated with CD8 T cell interleukin-21 production in HIV-1-infected individuals. *J Virol* 88:10259–10263.
42. Swaminathan S, Hu Z, Rupert AW, Higgins JM, Dewar RL, Stevens R, Chen Q, Rehm CA, Metcalf JA, Baseler MW, Lane HC, Imamichi T. 2014. Plasma interleukin-27 (IL-27) levels are not modulated in patients with chronic HIV-1 infection. *PLoS One* 9:e98989.
43. Kumar A, Abbas W, Herbein G. 2014. HIV-1 latency in monocytes/macrophages. *Viruses* 6:1837–1860.
44. Li Q, Li W, Yin W, Guo J, Zhang Z-P, Zeng D, Zhang X, Wu Y, Zhang X-E, Cui Z. 2017. Single-Particle Tracking of Human Immunodeficiency Virus Type 1 Productive Entry into Human Primary Macrophages. *ACS Nano* 11:3890–3903.
45. Kahn JO, Walker BD. 1998. Acute human immunodeficiency virus type 1 infection. *N Engl J Med* 339:33–39.
46. Bowers NL, Helton ES, Huijbregts RPH, Goepfert PA, Heath SL, Hel Z. 2014. Immune suppression by neutrophils in HIV-1 infection: role of PD-L1/PD-1 pathway. *PLoS Pathog* 10:e1003993.
47. Liu J, Zhan W, Kim CJ, Clayton K, Zhao H, Lee E, Cao JC, Ziegler B, Gregor A, Yue FY, Huibner S, MacParland S, Schwartz J, Song HH, Benko E, Gyenes G, Kovacs C, Kaul R, Ostrowski M. 2014. IL-10-producing B cells are induced early in HIV-1 infection and suppress HIV-1-specific T cell responses. *PLoS One* 9:e89236.

48. Frank AC, Zhang X, Katsounas A, Bharucha JP, Kottlilil S, Imamichi T. 2010. Interleukin-27, an anti-HIV-1 cytokine, inhibits replication of hepatitis C virus. *J Interferon Cytokine Res* 30:427–431.
49. Swaminathan S, Dai L, Lane HC, Imamichi T. 2013. Evaluating the potential of IL-27 as a novel therapeutic agent in HIV-1 infection. *Cytokine Growth Factor Rev* 24:571–577.
50. Henrick BM, Yao X-D, Rosenthal KL, INFANT study team. 2015. HIV-1 Structural Proteins Serve as PAMPs for TLR2 Heterodimers Significantly Increasing Infection and Innate Immune Activation. *Front Immunol* 6:426.
51. Greenhalgh AD, Zarruk JG, Healy LM, Baskar Jesudasan SJ, Jhelum P, Salmon CK, Formanek A, Russo MV, Antel JP, McGavern DB, McColl BW, David S. 2018. Peripherally derived macrophages modulate microglial function to reduce inflammation after CNS injury. *PLoS Biol* 16:e2005264.
52. Rodrigues V, Ruffin N, San-Roman M, Benaroch P. 2017. Myeloid Cell Interaction with HIV: A Complex Relationship. *Front Immunol* 8:1698.
53. Sweeney MD, Sagare AP, Zlokovic BV. 2018. Blood-brain barrier breakdown in Alzheimer disease and other neurodegenerative disorders. *Nat Rev Neurol* 14:133–150.
54. Keaney J, Campbell M. 2015. The dynamic blood–brain barrier. *FEBS J*.
55. Gomez-Nicola D, Perry VH. 2015. Microglial dynamics and role in the healthy and diseased brain: a paradigm of functional plasticity. *Neuroscientist* 21:169–184.
56. Menassa DA, Gomez-Nicola D. 2018. Microglial Dynamics During Human Brain Development. *Front Immunol* 9:1014.
57. Gertig U, Hanisch U-K. 2014. Microglial diversity by responses and responders. *Front Cell Neurosci* 8:101.
58. Rubin LH, Sacktor N, Creighton J, Du Y, Endres CJ, Pomper MG, Coughlin JM. 2018. Microglial activation is inversely associated with cognition in individuals living with HIV on effective antiretroviral therapy. *AIDS* 32:1661.
59. Rubio AE, Abraha A, Carpenter CA, Troyer RM, Reyes-Rodríguez ÁL, Salomon H, Arts EJ, Tebit DM. 2014. Similar replicative fitness is shared by the subtype B and unique BF recombinant HIV-1 isolates that dominate the epidemic in Argentina. *PLoS One* 9:e92084.
60. Hirsch VM, Olmsted RA, Murphey-Corb M, Purcell RH, Johnson PR. 1989. An African primate lentivirus (SIVsm) closely related to HIV-2. *Nature* 339:389–392.
61. Suzuki Y, Suzuki Y. 2011. Gene Regulatable Lentiviral Vector System. *Viral Gene Therapy*.

62. Scientists Identify Two Genes that “Shut Down” HIV-1 Virus.
63. Nkeze J, Li L, Benko Z, Li G, Zhao RY. 2015. Molecular characterization of HIV-1 genome in fission yeast *Schizosaccharomyces pombe*. *Cell Biosci* 5:47.
64. Forouzanfar F, Ali S, Wallet C, De Rovere M, Ducloy C, El Mekdad H, El Maassarani M, Aït-Ammar A, Van Assche J, Boutant E, Daouad F, Margottin-Goguet F, Moog C, Van Lint C, Schwartz C, Rohr O. 2019. HIV-1 Vpr mediates the depletion of the cellular repressor CTIP2 to counteract viral gene silencing. *Scientific Reports*.
65. Jain P, Boso G, Langer S, Soonthornvacharin S, De Jesus PD, Nguyen Q, Olivieri KC, Portillo AJ, Yoh SM, Pache L, Chanda SK. 2018. Large-Scale Arrayed Analysis of Protein Degradation Reveals Cellular Targets for HIV-1 Vpu. *Cell Rep* 22:2493–2503.
66. Usami Y, Wu Y, Göttlinger HG. 2015. SERINC3 and SERINC5 restrict HIV-1 infectivity and are counteracted by Nef. *Nature* 526:218–223.
67. Arizala JAC, Takahashi M, Burnett JC, Ouellet DL, Li H, Rossi JJ. 2018. Nucleolar Localization of HIV-1 Rev Is Required, Yet Insufficient for Production of Infectious Viral Particles. *AIDS Res Hum Retroviruses* 34:961–981.
68. Faust TB, Li Y, Bacon CW, Jang GM, Weiss A, Jayaraman B, Newton BW, Krogan NJ, D’Orso I, Frankel AD. 2018. The HIV-1 Tat protein recruits a ubiquitin ligase to reorganize the 7SK snRNP for transcriptional activation. *Elife* 7.
69. Ooms M, Letko M, Simon V. 2017. The Structural Interface between HIV-1 Vif and Human APOBEC3H. *J Virol* 91.
70. Stolp B, Fackler OT. 2011. How HIV takes advantage of the cytoskeleton in entry and replication. *Viruses* 3:293–311.
71. Dharan A, Campbell EM. 2018. Role of Microtubules and Microtubule-Associated Proteins in HIV-1 Infection. *J Virol* 92.
72. Wynn JE, Santos WL. 2015. HIV-1 drug discovery: targeting folded RNA structures with branched peptides. *Org Biomol Chem* 13:5848–5858.
73. Marin M, Kushnareva Y, Mason C, Chanda S, Melikyan G. 2019. HIV-1 Fusion with CD4 T cells Is Promoted by Proteins Involved in Endocytosis and Intracellular Membrane Trafficking. *Viruses*.
74. García-Expósito L, Ziglio S, Barroso-González J, de Armas-Rillo L, Valera M-S, Zipeto D, Machado J-D, Valenzuela-Fernández A. 2013. Gelsolin activity controls efficient early HIV-1 infection. *Retrovirology* 10:39.
75. Spear M, Guo J, Wu Y. 2012. The trinity of the cortical actin in the initiation of HIV-1 infection. *Retrovirology* 9:45.

76. Permanyer M, Pauls E, Badia R, Esté JA, Ballana E. 2013. The Cortical Actin Determines Different Susceptibility of Naïve and Memory CD4 T Cells to HIV-1 Cell-to-Cell Transmission and Infection. *PLoS ONE*.
77. Permanyer M, Pauls E, Badia R, Esté JA, Ballana E. 2013. The cortical actin determines different susceptibility of naive and memory CD4⁺ T cells to HIV-1 cell-to-cell transmission and infection. *PLoS One* 8:e79221.
78. Craveur P, Gres AT, Kirby KA, Liu D, Hammond JA, Deng Y, Forli S, Goodsell DS, Williamson JR, Sarafianos SG, Olson AJ. 2019. Novel Intersubunit Interaction Critical for HIV-1 Core Assembly Defines a Potentially Targetable Inhibitor Binding Pocket. *mBio*.
79. Márquez CL, Lau D, Walsh J, Shah V, McGuinness C, Wong A, Aggarwal A, Parker MW, Jacques DA, Turville S, Böcking T. 2018. Kinetics of HIV-1 capsid uncoating revealed by single-molecule analysis. *eLife*.
80. Novikova M, Zhang Y, Freed EO, Peng K. 2019. Multiple Roles of HIV-1 Capsid during the Virus Replication Cycle. *Virol Sin* 34:119–134.
81. Obr M, Kräusslich H-G. 2018. Viruses: The secrets of the stability of the HIV-1 capsid. *Elife* 7:e38895.
82. Mallery DL, Márquez CL, McEwan WA, Dickson CF, Jacques DA, Anandapadamanaban M, Bichel K, Towers GJ, Saiardi A, Böcking T, James LC. 2018. IP6 is an HIV pocket factor that prevents capsid collapse and promotes DNA synthesis. *Elife* 7.
83. Cosnefroy O, Murray PJ, Bishop KN. 2016. HIV-1 capsid uncoating initiates after the first strand transfer of reverse transcription. *Retrovirology* 13:58.
84. Rankovic S, Varadarajan J, Ramalho R, Aiken C, Rousso I. 2017. Reverse Transcription Mechanically Initiates HIV-1 Capsid Disassembly. *J Virol* 91.
85. Ehteshami M, Götte M. 2008. Effects of mutations in the connection and RNase H domains of HIV-1 reverse transcriptase on drug susceptibility. *AIDS Rev* 10:224–235.
86. Bejarano DA, Peng K, Laketa V, Börner K, Jost KL, Lucic B, Glass B, Lusic M, Müller B, Kräusslich H-G. 2019. HIV-1 nuclear import in macrophages is regulated by CPSF6-capsid interactions at the nuclear pore complex. *Elife* 8.
87. Deng H, Wang W, Yu J, Zheng Y, Qing Y, Pan D. 2015. Spectrin regulates Hippo signaling by modulating cortical actomyosin activity. *eLife*.
88. Wang G, Simon DJ, Wu Z, Belsky DM, Heller E, O'Rourke MK, Hertz NT, Molina H, Zhong G, Tessier-Lavigne M, Zhuang X. 2019. Structural plasticity of actin-spectrin membrane skeleton and functional role of actin and spectrin in axon degeneration. *eLife*.

89. Susuki K, Zollinger DR, Chang K-J, Zhang C, Huang CY-M, Tsai C-R, Galiano MR, Liu Y, Benusa SD, Yermakov LM, Griggs RB, Dupree JL, Rasband MN. 2018. Glial β II Spectrin Contributes to Paranode Formation and Maintenance. *J Neurosci* 38:6063–6075.
90. Han B, Zhou R, Xia C, Zhuang X. 2017. Structural organization of the actin-spectrin-based membrane skeleton in dendrites and soma of neurons. *Proc Natl Acad Sci U S A* 114:E6678–E6685.
91. Unsain N, Stefani FD, Cáceres A. 2018. The Actin/Spectrin Membrane-Associated Periodic Skeleton in Neurons. *Front Synaptic Neurosci* 10:10.
92. Bogusławska D, Machnicka B, Hryniewicz-Jankowska A, Czogalla A. 2014. Spectrin and phospholipids — the current picture of their fascinating interplay. *Cellular and Molecular Biology Letters*.
93. 3-Nov-2019. SPTBN1 spectrin beta, non-erythrocytic 1 [*Homo sapiens* (human)]. NCBI.
94. Kizhatil K, Davis JQ, Davis L, Hoffman J, Hogan BLM, Bennett V. 2007. Ankyrin-G is a molecular partner of E-cadherin in epithelial cells and early embryos. *J Biol Chem* 282:26552–26561.
95. Brown JW, Bullitt E, Sriswasdi S, Harper S, Speicher DW, McKnight CJ. 2015. The Physiological Molecular Shape of Spectrin: A Compact Supercoil Resembling a Chinese Finger Trap. *PLoS Comput Biol* 11:e1004302.
96. Horikoshi N, Pandita RK, Mujoo K, Hambarde S, Sharma D, Mattoo AR, Chakraborty S, Charaka V, Hunt CR, Pandita TK. 2016. β 2-spectrin depletion impairs DNA damage repair. *Oncotarget*.
97. Lodish, berk, Kaiser, Krieger, Bretscher, Ploegh, Amon, Scott. 2013. *molecular cell biology* 2:773–790.
98. Dominguez R, Holmes KC. 2011. Actin structure and function. *Annu Rev Biophys* 40:169–186.
99. Fletcher DA, Mullins RD. 2010. Cell mechanics and the cytoskeleton. *Nature* 463:485–492.
100. Tang DD, Gerlach BD. 2017. The roles and regulation of the actin cytoskeleton, intermediate filaments and microtubules in smooth muscle cell migration. *Respir Res* 18:54.
101. Lukic Z, Dharan A, Fricke T, Diaz-Griffero F, Campbell EM. 2014. HIV-1 uncoating is facilitated by dynein and kinesin 1. *J Virol* 88:13613–13625.
102. Huang P-T, Summers BJ, Xu C, Perilla JR, Malikov V, Naghavi MH, Xiong Y. 2019. FEZ1 Is Recruited to a Conserved Cofactor Site on Capsid to Promote HIV-1 Trafficking. *Cell Reports*.

103. He S, Fu Y, Guo J, Spear M, Yang J, Trinité B, Qin C, Fu S, Jiang Y, Zhang Z, Xu J, Ding H, Levy DN, Chen W, Petricoin E 3rd, Liotta LA, Shang H, Wu Y. 2019. Cofilin hyperactivation in HIV infection and targeting the cofilin pathway using an anti- $\alpha 4\beta 7$ integrin antibody. *Sci Adv* 5:eaat7911.
104. Cooper J, Liu L, Woodruff EA, Taylor HE, Goodwin JS, D'Aquila RT, Spearman P, Hildreth JEK, Dong X. 2011. Filamin A protein interacts with human immunodeficiency virus type 1 Gag protein and contributes to productive particle assembly. *J Biol Chem* 286:28498–28510.
105. Shin Y, Choi B-S, Kim K-C, Kim K, Yoon C-H. 2019. Diverse Effects of Small Molecule Inhibitors on Actin Cytoskeleton Dynamics in HIV-1 Infection. *J Bacteriol Virol* 49:69–80.
106. Ingram Z, Taylor M, Okland G, Martin R, Hulme AE. 2020. Characterization of HIV-1 uncoating in human microglial cell lines. *Virol J* 17:31.
107. Janabi N, Peudenier S, Héron B, Ng KH, Tardieu M. 1995. Establishment of human microglial cell lines after transfection of primary cultures of embryonic microglial cells with the SV40 large T antigen. *Neurosci Lett* 195:105–108.
108. Hulme AE, Hope TJ. 2014. The cyclosporin A washout assay to detect HIV-1 uncoating in infected cells. *Methods Mol Biol* 1087:37–46.
109. Cavrois M, Neidleman J, Greene WC. 2014. HIV-1 Fusion Assay. *Bio Protoc* 4.
110. Burdick RC, Li C, Munshi M, Rawson JMO, Nagashima K, Hu W-S, Pathak VK. 2020. HIV-1 uncoats in the nucleus near sites of integration. *Proc Natl Acad Sci U S A* 117:5486–5493.
111. Falk W, Goodwin RH Jr, Leonard EJ. 1980. A 48-well micro chemotaxis assembly for rapid and accurate measurement of leukocyte migration. *J Immunol Methods* 33:239–247.